Multilocus phylogeography of the common midwife toad, *Alytes obstetricans* (Anura, Alytidae): contrasting patterns of lineage diversification and genetic structure in the Iberian refugium

H Gonçalves[1], B Maia-Carvalho[1,2], T Sousa-Neves[1,3], M García-París[4], F Sequeira[1], N Ferrand[1,2,5], I Martínez-Solano[1,6,7]

[1] *CIBIO Research Centre in Biodiversity and Genetic Resources, InBIO, Universidade do Porto, Campus Agrário de Vairão, 4485-661 Vairão, Portugal*

[2] *Departamento de Biologia, Faculdade de Ciências da Universidade do Porto, 4099-002 Porto, Portugal*

[3] *Museu Paraense Emílio Goeldi, Caixa Postal 399, Belém, PA 66040-170, Brazil*

[4] *Museo Nacional de Ciencias Naturales, MNCN-CSIC, c/ José Gutiérrez Abascal 2, 28006 Madrid, Spain*

[5] *Department of Zoology, University of Johannesburg, Johannesburg, South Africa*

[6] *Instituto de Investigación en Recursos Cinegéticos (CSIC-UCLM-JCCM), Ronda de Toledo, s/n, 13005 Ciudad Real, Spain*

[7] *Ecology, Evolution and Development Group, Department of Wetland Ecology, Estación Biológica de Doñana (EBD-CSIC), Avenida Américo Vespucio, s/n, 41092 Sevilla, Spain*

Corresponding author: E-mail: hgoncalves@cibio.up.pt. Present address: CIBIO Research Centre in Biodiversity and Genetic Resources, InBIO, Universidade do Porto, Campus Agrário de Vairão, 4485-661 Vairão, Portugal. Phone: +351 252 660 411 ext. 270; Fax: +351 252 661 780.

1

Abstract

Recent investigations on the evolutionary history of the common midwife toad (*Alytes obstetricans*) revealed high levels of geographically structured genetic diversity but also a situation where delineation of major historical lineages and resolution of their relationships are much more complex than previously thought. We studied sequence variation in one mitochondrial and four nuclear genes throughout the entire distribution range of all recognized *A. obstetricans* subspecies to infer the evolutionary processes that shaped current patterns of genetic diversity and population subdivision. We found six divergent, geographically structured mtDNA haplogroups diagnosing population lineages, and varying levels of admixture in nuclear markers. Given the timeframe inferred for the splits between major lineages, the climatic and environmental changes that occurred during the Pleistocene seem to have shaped the diversification history of *A. obstetricans*. Survival of populations in allopatric refugia through the Ice Ages supports the generality of the "refugia-within-refugia" scenario for the Iberian Peninsula. However, lineages corresponding to subspecies *A. o. almogavarii*, *A. o. pertinax*, *A. o. obstetricans,* and *A. o. boscai* responded differently to Pleistocene climatic oscillations after diverging from a common ancestor. *Alytes o. obstetricans* expanded northward from a northern Iberian refugium through the western Pyrenees, leaving a signal of contrasting patterns of genetic diversity, with a single mtDNA haplotype north of the Pyrenees from SW France to Germany. Both *A. o. pertinax* and *A. o. boscai* are widespread and genetically diverse in Iberia, the latter comprising two divergent lineages with a long independent history. Finally, *A. o. almogavarii* is mostly restricted to the north-eastern corner of Iberia north of the Ebro river, with additional populations in a small region in south-eastern France. This taxon exhibits unparalleled levels of genetic diversity and little haplotype sharing with other lineages, suggesting a process of incipient speciation.

Introduction

Patterns of genetic diversity within species are a consequence of their evolutionary history and of contemporary constraints to dispersal, and these processes are expected to give rise to specific phylogeographic patterns (Avise, 2000, 2009). The detection and description of these patterns are the key to infer the evolutionary history of a species, and this knowledge has important implications for predicting biotic responses to current and future periods of global climate change, and ultimately, to provide valuable information for the conservation and management of species and populations (Moritz and Agudo, 2013; Velo-Antón et al., 2013; Fordham et al., 2014).

In the last three decades, numerous phylogeographic studies have shown that Quaternary climatic oscillations caused severe range shifts in species distributions and have been among the most important historical factors in shaping the genetic structure of temperate species (Taberlet et al., 1998; Hewitt, 2000, 2004). It is well known that Southern Europe, including the peninsulas of Iberia, Italy, and the Balkans, has functioned as a refugial area for temperate species survival during periods of adverse climatic conditions (Taberlet et al., 1998; Hewitt, 2001; Stewart et al., 2010). Geographical separation and long-lasting persistence in these refugia caused divergence of local populations and the evolution of genetic lineages or even speciation (Hewitt, 1996). High genetic diversity can often be detected in populations located in former refugia (Hewitt, 2000, 2004), while populations at the leading edge of a species' distribution are mostly characterized by lower genetic diversity (Hampe and Petit, 2005; Recuero and García-París, 2011). Within the Iberian Peninsula, a geologically and ecologically complex and heterogeneous region, multiple population-divergence processes across different geographical and temporal scales have been described for a variety of taxa, showing the existence of "refugia within refugia" (Gómez and Lunt, 2007; Abellán and Svenning,

4

2014). Characterizing these refugial areas is of the utmost importance for the long-term conservation of species and populations, since they frequently harbour most of the species' genetic diversity and thus their potential to cope with environmental changes (Hampe and Petit, 2005; Schoville et al., 2012; Dufresnes et al., 2013).

The common midwife toad, *Alytes obstetricans* (Laurenti, 1768) is widely distributed in Western Europe, from Germany to the northern half of the Iberian Peninsula (Fig. 1; Grossenbacher, 1997). However, most of the species' genetic diversity is found in Iberia (Maia-Carvalho et al., 2014a). Currently, four subspecies are recognized within *A. obstetricans* (Fig. 1): *i*) *A. o. obstetricans* (Laurenti, 1768), distributed across western Europe and the northern Iberian Peninsula (Navarra, Basque Country and Cantabrian Mountains); *ii*) *A. o. boscai* Lataste, 1879, in northern and central Portugal, Galicia, western Castilla-León as well as along the Sistema Central mountains; *iii*) *A. o. pertinax* García-París and Martínez-Solano, 2001, present in the central and eastern regions of the Iberian Peninsula (García-París and Martínez-Solano, 2001); and *iv*) *A. o. almogavarii* Arntzen and García-París, 1995, distributed from the eastern Pyrenees (Geniez and Crochet, 2003) up to the Sierra de Guadarrama, north of Madrid (García-París, 1995). According to Arntzen & García-París (1995) and Martínez-Solano *et al*. (2004), the differentiation between subspecies may be related to the formation of the main fluvial drainages in the Iberian Peninsula, about 4 Mya (millions of years ago) or, alternatively, be associated with isolation in different Pleistocene glacial refugia. While several studies have addressed patterns of variation in morphology, allozymes, and mitochondrial and nuclear DNA (Arntzen and García-París, 1995; Fonseca et al., 2003; Martínez-Solano et al., 2004; Gonçalves et al., 2007), several aspects of the evolutionary history of this species remain unsolved. Recently, a study by Maia-Carvalho et al. (2014a), based on mitochondrial and microsatellite data in a set of populations representative of all currently recognized

subspecies, revealed discordances with previous studies. First, the location of the northern boundary between *A. o. boscai* and *A. o. obstetricans* had been inferred to be in the Pyrenees, based on allozyme data (Arntzen and Szymura, 1984), but was shown to be more likely located in the Iberian northwest, somewhere between northern Portugal and the Cantabrian Mountains. Second, Maia-Carvalho et al. (2014a) revealed the existence of two well-differentiated groups within *A. o. boscai*, separated by the Douro River, as suggested by Fonseca et al. (2003). Additionally, the recent multilocus assessment of phylogenetic relationships in *Alytes* by Maia-Carvalho et al. (2014b) produced inconclusive results about the relationships between major clades in *A. obstetricans* and indicated conflict with the current morphology-based subspecific taxonomy.

In this study, we use a range-wide multilocus dataset (one mitochondrial and four nuclear genes) to investigate further the evolutionary history of *A. obstetricans*, with special interest in patterns of population subdivision and postglacial expansion. Specifically, we assess the extent of mutual compatibility between nuclear and mitochondrial markers and the relationship with previously described morphological subspecies, and the dynamics of population fragmentation, differentiation and post-glacial expansion. We discuss the evolutionary processes that may have acted as drivers of diversification and the taxonomic and conservation implications of our results.

Material and methods

Sampling and DNA extraction

We analysed 227 common midwife toads from 103 sampling sites spread across the species' entire geographical range (Fig. 1, Table 1). Our sampling scheme was designed to incorporate individuals from all recognized subspecies, including their type localities when possible (Fig. 1). Some mitochondrial and nuclear sequences (identified in Table 1) were generated in previous genetic studies on *Alytes* (Gonçalves et al., 2007; Gonçalves et al., 2009; Pinho et al., 2010; Maia-Carvalho et al., 2014a, b). Newly collected tissue samples were obtained from toe tips of adults or tail tips of larvae, and preserved in 95% ethanol. All individuals were released *in situ*. Whole genomic DNA was extracted following the standard high-salt protocol of Sambrook et al. (1989) or using EasySpin Genomic DNA Minipreps Tissue Kit (SP-DT-250, Qiagen, Hilden, Germany) following the manufacturer's protocol.

Amplification, sequencing and haplotype determination

Five gene regions including one mitochondrial fragment of the NADH dehydrogenase subunit 4 gene and adjacent tRNAs (hereafter referred to as *ND4*) and four nuclear genes (β-fibrinogen intron 7 - *ß-fibint7*; Protein phosphatase 3, catalytic subunit, alpha isoform intron 4 – *PPP3CAint4*; Ribosomal protein L9 intron 4 – *RPL9int4*; and a segment of exon 2 and intron 2 of the cellular myelocytomatosis proto-oncogene - *C-myc*) were amplified via polymerase chain reaction (PCR).

The following primers were used for amplification and sequencing: for *ND4* - primers *ND4* and *Leu* (Arévalo et al., 1994); for *ß-fibint7* a two-step amplification procedure was used, with a combination of two primer pairs - PCR1: *FIBX7* and *FIBX8*; PCR2: *BFXF* and *BFXR* (Sequeira et al., 2006); for *PPP3CAint4* - primers *PPP3CA4F1*

and *PPP3CA5R1* (Pinho et al., 2010); for *RPL9int4* - *RPL94F* and *RPL95R* (Pinho et al., 2010); and for *C-myc* - primers *Cmyc1U* (Crawford, 2003) and *Cmyc3cat* (Brunes et al., 2010). PCRs were carried out in 10 µl volume containing 1x PCR buffer (50 mm Tris–HCl, 50 mm NaCl, pH 8.5); 3 mM MgCl2; 0.4 mM each dNTPs, 0.5U of Phusion High-Fidelity PCR Master Mix (Thermo Scientific), 0.3 µM each primer and approximately 50 ng of genomic DNA. For *ND4* and *ß-fibint7* amplification conditions were those described in Gonçalves et al. (2007). For *PPP3CAint4*, *RPL9int4* and *C-myc* amplification conditions followed Maia-Carvalho et al. (2014b). Purified products of each reaction were sequenced with the ABI Prism BigDye Terminator v3.1 Sequencing Kit protocol on an ABI3130xl DNA analyzer (Applied Biosystems, Foster City, California, USA). All sequences generated for this study are deposited in GenBank under Accession Numbers KT363119-KT363648 (Table 1).

Sequences were assembled with the software ChromasPro v1.5 (www.technelysium.com.au/ChromasPro.html). The assembled sequences were then edited and aligned manually using the program BioEdit v7.1.3.0 (Hall, 1999).

Polymorphic positions of *ß-fibint7*, *PPP3CAint4*, *RPL9int4* and *C-myc* corresponding to heterozygous individuals were coded with IUPAC ambiguity codes. For each input genotype sequence of heterozygous individuals, we inferred phased haplotypes probabilistically through the Bayesian algorithm implemented in PHASE v2.1.1 (Stephens et al., 2001; Stephens and Donnelly, 2003), using SeqPHASE (Flot, 2010) to format the input files. In the four nuclear loci we detected single and multiple-base insertions or deletions (indels). For phasing analyses we pruned the data assuming that indels likely resulted from a single evolutionary step. We left only the first base of the indel (in the case of an insertion) or reduced them to one single step (deletion). We choose this approach rather than completely removing indels because this would significantly reduce the number

of polymorphic sites and disregard some of the information contained in the data sets. Heterozygous indels, which resulted from the amplification of alleles of different sizes in a single individual, were decoded interpreting directly the mixed trace formed by the two allelic peaks superimposed onto each other downstream of the indel (Sousa-Neves et al., 2013). All known haplotypes were incorporated for subsequent haplotype inference. We ran PHASE three times with different random seeds and checked if haplotype estimation was consistent across runs. Each run was conducted using default values. We used a threshold of 0.90 posterior probability to accept a given haplotype phase reconstruction.

Data analysis

A gene tree for the mtDNA marker *ND4* was reconstructed using maximum likelihood (ML) and Bayesian inference (BI) analyses. The most appropriate model of nucleotide evolution was selected using PartitionFinder v1.1.0 (Lanfear et al., 2012) under the Akaike information criterion (AIC; Akaike, 1973). ML analyses were performed with the software RAxML v7.2.8 (Silvestro and Michalak, 2010), using the graphical front-end RAx-ML GUI v1.1 (Randomized Axelerated Maximum Likelihood; Stamatakis, 2006). Through the bootstrap option, ML analyses were run ten times from starting random seeds to generate 1000 nonparametric bootstrap replicates. Bayesian analyses were performed in the version of MrBayes v3.1.2 hosted at the CIPRES Science Gateway Portal v3.1 (San Diego Supercomputer Center; Miller et al., 2010; http://www.phylo.org/portal/), using two replicate searches with $10x10^7$ generations each and sampling every 10,000th generations. Four MCMC (Markov chain Monte Carlo) were run simultaneously in each analysis. Stationarity for each run was detected through three different ways. First, we assessed the convergence among chains by plotting the log-likelihood values against generation number using Tracer v1.6 (Rambaut et al., 2014). Secondly, we used the online program AWTY

(Nylander et al., 2008) to analyze the trace plot of the log-likelihood and the cumulative split frequencies across all post-burn-in generations within each analysis. Finally, we checked the standard deviation of split frequencies as a convergence index (<0.001). After assessing chain convergence, we discarded all samples obtained during the first ten million generations as burn-in. Post-burn-in trees from all replicates were combined estimating a 50% majority-rule consensus tree. The frequency of any particular clade in the consensus tree represents the posterior probability of that clade (Huelsenbeck and Ronquist, 2001).

To test for recombination in nuclear loci we used the difference in sums of squares (DSS) method as implemented in software TOPALi v2.5 (Milne et al., 2004), with a sliding window of 100-bp and 10-bp step size.

Genealogical relationships among haplotypes (haplotype networks) for each locus were estimated using phylogenetic algorithms with proper models of sequence evolution, as implemented in Haploviewer (Salzburger et al., 2011). Phylogenetic reconstructions among haplotypes for each locus were estimated using a Maximum Likelihood (ML) approach, as implemented in the software RAxML. Using default options, we ran the program with the best-fit model for each locus as selected by PartitionFinder, and the generated trees were used to estimate each haplotype network.

For both mtDNA and nuclear fragments genetic diversity parameters were estimated using DnaSP v5.10 (Librado and Rozas, 2009). We also used DnaSP to perform a pairwise mismatch-distribution analysis (Rogers and Harpending, 1992), and to calculate Fu's Fs (Fu, 1997), Tajima's D (Tajima, 1989) and Ramos-Onsins & Rozas' R2 (Ramos-Onsins and Rozas, 2002) statistics, in order to test for molecular signatures of demographic expansion. Genetic distances (p-uncorrected) within and between lineages were calculated with MEGA v5 (Tamura et al., 2011). Additionally, we performed an Extended Bayesian Skyline Plot (Heled and Drummond, 2008) analysis using all available sequences for *A.*

obstetricans (*ND4*: 210; *ß-fibint7:* 169*; C-myc:* 30*; PPP3CAint4:* 38*; and RPL9int4:* 41*;* numbers refer to individuals, and for nuclear markers the number of sequences is twice that number because there are two copies for each individual). This coalescent-based analysis estimates the effective population size (*Ne*) through time and is implemented in BEAST v.1.8 (Drummond et al., 2012). Optimal nucleotide-substitution models were selected by jModeltest v2.1 (Darriba et al., 2012). For models incorporating both gamma-distributed rate variation (+G) and proportion of invariant sites (+I) we implemented only +G with 10 rate categories due to the computational difficulty of simultaneously estimating both +G and +I.

We analyzed our multilocus dataset under the multispecies coalescent as implemented in *BEAST v1.8 (Heled and Drummond, 2010). The alignments included *ND4* sequences of 174 individuals, and phased nuclear sequences (two alleles per individual) for 27 (*C-myc*), 35 (*PPP3CAint4*), 35 (*RPL9int4*), and 140 (*ß-fibint7*) individuals. We defined five independent partitions, one for each marker. The optimal substitution models for each partition were selected by jModeltest. Molecular clocks (strict for all partitions) and tree priors were unlinked across partitions. As species-tree prior, we used the Yule speciation model. We used samples of all extant *Alytes* species, including *A. cisternasii, A. muletensis, A. dickhilleni* and *A. maurus* as outgroups in the analyses. We also defined six groups in *A. obstetricans* corresponding to the six major population lineages identified in previous analyses (A-F, see Results). Samples from the three localities where two mtDNA haplotype clades were found in sympatry (22, 43, and 89) were excluded from the analyses since *BEAST does not take into account the possibility of gene flow across lineages. Additionally, we also excluded individuals from localities where gene flow was suspected because of geographical proximity and/or patterns of nuclear haplotype sharing. Localities excluded from this analysis for this reason included 6, 16, 19, 23, 28, 31-36, 44-48, 62-63,

11

and 102. In the absence of prior information about clock rates for the markers used, we performed an additional phylogenetic analysis on a reduced *ND4* dataset including representatives of all major mtDNA haplogroups within *A. obstetricans* (sample codes: ALB1, BER6, HUE1, MNCN8590, SMA25, and TIN1, see Table 1), all other species of *Alytes* (*A. cisternasii* CER17; *A. muletensis* IMS3517; *A. maurus* MAR01; and *A. dickhilleni* IMS3489)*,* and sequences of the related genera *Discoglossus* and *Bombina* downloaded from GenBank (*Discoglossus galganoi* AY442088; *D. jeanneae* AY442115; *D. pictus* AY442137; *D. scovazzi* AY442139; *Bombina bombina* JX893173; *B. variegata* AY971143; *B. variegata* JX893176; *B. variegata* JX893179; *B. orientalis* AY585338; *B. microdeladigitora* JX893182; and *B. maxima* JX893181) (Martínez-Solano, 2004; San Mauro et al., 2004; Pabijan et al., 2013). This reduced dataset was analyzed as a single partition in BEAST, with the optimal substitution model selected by jModeltest. We used the Yule speciation prior with a strict clock and calibrated the node separating eastern and western Palearctic *Bombina* species following Pabijan et al. (2013), with a logNormalPrior encompassing values between 13.4 and 32.2 Mya (mean = 0.994, st. dev. = 1, offset = 13.0, meanInRealSpace = false). The mean and 95% Highest Posterior Density interval (95% HPD) estimated in this analysis for the parameter "clock rate" were subsequently used to specify a normal prior for the *ND4* clock rate in the *BEAST analysis (mean: 0.0085, st. dev. = 0.002), with diffuse Gamma priors (shape: 0.01, scale: 100) for the clock rates of nuclear markers. Species-tree analyses were run for 200 million generations, and the logfile was inspected in Tracer to assess adequate mixing and convergence. All effective sample sizes (ESS) of parameters estimated were well >200, as recommended by the authors of the software. A burn-in period of 10% of the total running time was specified after trace inspection, and a Maximum Clade Credibility consensus tree was constructed with the program TreeAnnotator, which is distributed as part of the BEAST

package. A similar analysis, but excluding the mtDNA partition was also run to test for the effect of mtDNA on the species tree (see for instance Jockusch et al., 2015).

Results

The mitochondrial DNA alignment consisted of 210 sequences of 813 base pairs (bp) yielding 88 haplotypes defined by 138 polymorphic sites, of which 127 were parsimony informative (Table 2). For the nuclear dataset we obtained 338 sequences with 630–635 bp for *ß-fibint7*, 76 sequences with 597–604 bp for *PPP3CAint4*, 82 sequences with 442-460 bp for *RPL9int4*, and 60 sequences with 1257-1261 bp for *C-myc* (Table 2). In the *ß-fibint7* alignment, 57 out of 59 polymorphic sites were parsimony informative. For *PPP3CAint4*, 22 out of 26 polymorphic sites were parsimony informative. For *RPL9int4* and *C-myc*, 27 and 24 out of 29 and 26 polymorphic sites were parsimony informative, respectively. We did not find significant evidence of recombination in the nuclear markers.

Phylogenetic analyses of mtDNA sequences recovered a well-resolved tree with six major haplotype clades (labeled A to F, Fig. 2), with a strong association with geography (Fig. 1), diagnosing six population lineages. Briefly, haplogroup A (blue in the figures) corresponds to populations of *A. o. pertinax* but extends much further than previously thought, along the Iberian northern plateau up to the Cantabrian Mountains and in the east end of the Central System mountains (Sierras de Guadarrama and Ayllón), filling most of the region not ascribed to any subspecies in previous studies; haplogroup B (yellow) corresponds to populations of *A. o. obstetricans* and extends from northern Spain (Cantabrian Mountains) to central Europe and also to the west, up to Galicia; haplogroup C (red) corresponds to populations of *A. o. boscai* and occurs in Galicia and northwest Portugal; haplogroup D (green) includes all Portuguese populations south of the Douro River and the Spanish populations from the western part of the Central System (Sierras de

Gata and Gredos, traditionally considered as part of *A. o. boscai*); haplogroup E (gray) was only detected in populations of the Spanish central Pyrenees, while haplogroup F (orange) corresponds to populations of *A. o. almogavarii*. Haplogroup D is the sister taxon to a clade comprising the other five haplogroups (BPP: 1.0), and haplogroups A, B and C form a monophyletic group (BPP: 1.0). In three populations, we found haplotypes of different haplogroups co-occurring (Table 2 and Fig. 1). These include localities 22 (haplogroups B+C), 43 (haplogroups A+B) and 89 (haplogroups A+F).

Haplotype networks based on mtDNA and nuclear sequences are presented in Fig. 3. The mtDNA haplotype genealogy showed the same six groups as the phylogenetic tree. Within each haplogroup, the most frequent haplotypes generally show an interior position, whereas the remaining are in most cases closely connected by one-step mutations. Haplogroups C and D exhibit star-like topologies, with one high frequency, central haplotype and several additional haplotypes connected by few-step mutations, suggesting recent demographic expansion. The most frequent haplotype in haplogroup C is present in 14 out of 23 sequences and is widely distributed, with 9 haplotypes occurring only once. The most frequent haplotype in haplogroup D occurs in 7 out of 19 individuals from the Iberian Central System, with 12 haplotypes with a frequency of 1. In haplogroup B the most frequent haplotype (frequency=7) is almost exclusive of the French and German populations. We found a total of 18 haplotypes in this haplogroup, with frequencies ranging from 1-7. Haplogroup A has several frequent haplotypes that are widely distributed. We found 34 haplotypes in this haplogroup, with a highest frequency of 14, and 22 haplotypes observed only once. The most frequent haplotype in haplogroup F occurs in 16 out of 36 individuals and is widely distributed through Catalonia. Finally, haplogroup E is represented by a single haplotype. The nuclear networks were generally compatible with mtDNA in the diagnosis of six major population lineages, with similar

14

results for each of the four genes (Fig. 3). In the *C-myc* network, all population lineages had non-overlapping sets of haplotypes, whereas the other three nuclear networks (*ß-fibint7*, *PPP3CAint4* and *RPL9int4*) showed the presence of heterozygous individuals with alleles characteristic of different inferred population lineages (Figs 1, 3).

Measures of genetic diversity for the mitochondrial gene and the four nuclear loci are summarized in Table 2. We found high levels of genetic diversity in *A. obstetricans* (π *ND4* = 0.0243; π *β-fibint7* = 0.0155; π *RPL9int4* = 0.0124; π *PPP3CAint4* = 0.0075; π *C-myc* = 0.0035). The mitochondrial average genetic distance (p-uncorrected) ranged from 5.2% between haplotype clades D and F to 1.4% between haplotype clades B and C (Table 3). Within haplogroups, p-distances were higher in haplogroups B and C (0.70%) than in the other haplogroups (0.00-0.40%, Table 3).

Significant values of Fu's Fs and Ramos-Onsins & Rozas' R2 statistics were obtained for the population lineages corresponding to mtDNA haplogroups A, C and D (Table 2). Tajima's D statistic was also significant for the population lineage corresponding to mtDNA haplogroup C. Mismatch distributions showed similar patterns, supporting scenarios of demographic expansion in the population lineages A, C and D (Fig. 4). The EBSP showed a sustained increase in *Ne* through the Pleistocene and up to the present (Fig. 5).

Species-tree analyses recovered largely unresolved topologies (Fig. 6), with lineage F as the sister taxon to a clade comprising the other five lineages but with low support (BPP<0.9), with only lineage A being recovered as the sister taxon to lineage B (BPP: 0.99). Estimates of split times were calculated for several nodes in the species-tree, with median values for the root of 21.1 Mya (95% HPDi: 10.1-37.9), 5.6 Mya (95% HPDi: 3.0-9.8 for the basal split in *Baleaphryne* (the clade that includes *A.dickhilleni*, *A. maurus* and *A. muletensis*), and 2.5 Mya for the basal split in *A. obstetricans*, separating lineage F from

the rest (95% HPDi: 1.4-4.3). Thus, the splits between the six major population lineages in

A. obstetricans date back to the Pleistocene, although their relative splitting order is

unresolved (Fig. 6). The same largely unresolved topology was recovered in analyses

based on the four nuclear markers, with a weakly supported basal split separating lineage F

from the rest (BPP: 0.87) and strong support for a sister-group relationship between

lineages A and B (BPP: 0.99).

Discussion

Our analysis of genetic diversity in *A. obstetricans* revealed very high levels of

intraspecific variation in Iberia, in agreement with previous results based on allozymes

(Arntzen and García-París, 1995), morphology (Martínez-Solano et al., 2004), and mtDNA

and nuclear markers (Fonseca et al., 2003; Martínez-Solano et al., 2004; Gonçalves et al.,

2007; Maia-Carvalho et al., 2014a). The common midwife toad has been previously

considered as including four essentially parapatric subspecies in the Iberian Peninsula (*A.

o. obstetricans*, *A. o. boscai*, *A. o. pertinax,* and *A. o. almogavarii*; see Fig. 1 for their

respective geographical distributions), but our study shows additional and different

patterns of genetic subdivision and allows finer delineation of their ranges. Based on

mtDNA data, both the phylogenetic tree and the haplotype genealogy clearly recovered six

different haplogroups, three of which are highly divergent (D, E and F, with average p-

uncorrected distances with other haplogroups of 4.4%, 3.7%, and 4.7%, respectively, see

Table 3). These mtDNA haplogroups diagnose six population lineages with very strong

geographical concordance: only in three locations we documented the presence of more

than one lineage (Fig. 1). Although the nuclear genealogies are in general mutually

compatible with mtDNA data, they do not recover monophyly of the six mtDNA-defined

haplogroups. Probably this result reflects the retention of ancestral polymorphisms in the slowest-evolving markers.

Our species-tree analysis recovered largely unresolved trees (Fig. 6), which may be a consequence of insufficient resolution in the markers used or of nearly simultaneous divergence across population lineages. Nevertheless, the species tree recovered lineage F as the sister taxon to a clade comprising the other five extant lineages, albeit with low support (BPP: 0.78 in the combined vs BPP: 0.87 in the nuclear species tree). Lineage F includes populations previously ascribed to *A. o. almogavarii*, and was estimated to diverge from the other lineages around 2.5 Mya (1.4-4.3). The combined evidence from mtDNA and nuclear markers suggests that *A. o. almogavarii* is an ancient form restricted to the north-eastern corner of the Iberian Peninsula, where it persisted probably since the Pleistocene. Its presence in SE France, anticipated by Geniez and Crochet (2003), was confirmed in our study, but the contact zone with *A. obstetricans* in France remains to be described in detail in future studies. Apparently, this lineage does not cross the Ebro valley, in contradiction with previous results that suggested an extended geographical distribution reaching the mountains of Guadarrama, close to Madrid (García-París, 1995). Our results also contradict the initial hypothesis of García-París (1995), later expanded by Martínez-Solano et al. (2004) and Gonçalves et al. (2007), suggesting that *A. o. almogavarii* might have been a highly divergent lineage that progressively lost its genetic identity due to extensive hybridization and introgression with its neighbouring lineages. On the contrary, the high diversity, overall concordance across markers, with little allele sharing with other lineages, and geographical confinement of *A. o. almogavarii* suggests that it may represent an incipient species. However, potential changes in its specific taxonomic status must await further studies focusing on admixture patterns in the putative contact zones with both *A. o. obstetricans* and *A. o. pertinax* that have been revealed in this

study, as well as in other as yet understudied areas, in order to assess the extent of reproductive isolation across lineages.

While the range of *A. o. almogavarii* apparently remained stable for a long period of time within a restricted area, the other extant *A. obstetricans* subspecies may have expanded and contracted multiple times. Given the inferred timeframe for the split between lineage F and these lineages, it is likely that these demographic fluctuations were associated with the climatic oscillations that characterized the Pleistocene. Lineage D includes populations south of the Douro River in Portugal and along the western part of the Sistema Central mountains in central Iberia, previously assigned to subspecies *A. o. boscai*. This finding confirms previous results based on mtDNA and microsatellite data (Fonseca et al., 2003; Maia-Carvalho et al., 2014a), which highlighted the genetic distinctiveness of these populations. The mountains south of the Douro are well-known hotspots of genetic diversity and correspond to important glacial refugia where many different species have persisted across the Ice Ages (e.g. Alexandrino et al., 2000; Paulo et al., 2001; Martínez-Solano et al., 2006). Lineage C is restricted to north-western Iberia and includes the type locality of *A. o. boscai* (Tuy, in the province of Pontevedra, Spain; see García-París and Martínez-Solano, 2001). The pattern of mtDNA haplotype diversity and significant values of Tajima's D and Ramos-Onsins & Rozas' R^2 statistics suggest a rapid and recent expansion, consistent with the results of the mismatch distribution analysis. Further research is needed to delineate the contact zone with lineage B, although the finding of haplotypes of both lineages (B+C) co-occurring in locality 22 (Arteixo, A Coruña - Table 1 and Fig. 1) is in accordance with previous descriptions of the geographical border between the two subspecies, which was located in the western slopes of the Cantabrian Mountains in Galicia, based on allozymes and colouration patterns (Arntzen and García-París, 1995).

The results from both mtDNA and nuclear genealogies show that lineage A corresponds to subspecies *A. o. pertinax* (García-París and Martínez-Solano, 2001). However, its current range is much more extensive than previously considered, occupying, to the north, the southern margin of the Ebro River up to the Cantabrian Mountains and, to the west, the Spanish-Portuguese border. Both mtDNA and nuclear data suggest the occurrence of a contact zone between this subspecies and *A. o. almogavarii* in the northeast, with *A. o. obstetricans* in the north and north-west, and with *A. o. boscai* in the west (Sierra de Gata), respectively (Fig. 1). Thus, high-elevation (>2,000 m) habitats in the Estrela and Gredos mountains (western Central System) and Guadarrama (eastern Central System) seem to have been colonized independently by lineages corresponding to part of subspecies *A. o. boscai* (the highly divergent lineage D) and subspecies *A. o. pertinax,* respectively. Similarly, the high-elevation mountain habitats in the north have been independently colonized by subspecies *A. o. obstetricans* (Cantabrian mountains) and *A. o. almogavarii* (Pyrenees). Since these populations are those most heavily affected by chytridiomycosis-related mass mortality events, taking into account the phylogenetic affinities of extirpated and potential source populations with no record of massive die-offs will be critical to plan successful captive breeding and reintroduction. The susceptibility to disease (bacteria, chytrid fungi, ranaviruses) of high-elevation populations in four of the six major population lineages identified in our study (Márquez et al., 1995; Bosch et al., 2001; Walker et al., 2010; Rosa et al., 2012; Price et al., 2014) favours environmental correlates as explanatory variables in population die-offs and dismisses the role of potential historical factors derived from a shared evolutionary history. However, genetic bottlenecks associated with the colonization of high-elevation habitats probably also represent a contributing factor (Albert et al., 2014).

19

Finally, lineage B (*A. o. obstetricans*) extends from Northern Spain to Central Europe. North of the Pyrenees, the large geographical area occupied by this lineage (comprising France, Luxembourg and parts of Germany, Netherlands, Switzerland and Belgium) is almost depleted of genetic variation, as shown by the reduced haplotypic diversity, suggesting a rapid and recent expansion from the southern slopes of the western Pyrenees, probably after the Last Glacial Maximum. In contrast, populations south of the Pyrenees show considerable levels of both mtDNA and nuclear diversity. Contrasting patterns of genetic diversity cannot be attributed to biases in our sampling, where populations north of the Pyrenees are under-represented, but sampling effects may explain lack of significant results in neutrality tests. This pattern of contrasting diversity south and north of the Pyrenees and the inferred colonization route resemble those described for other amphibian species, such as *Lissotriton helveticus* (Recuero and García-París, 2011).

Taken together with phylogenetic results, both genetic diversity and phylogeographical data provide compelling evidence that the Iberian Peninsula has served as a long-term refugium for *A. obstetricans*. In fact, our results indicate that ancestral *A. obstetricans* populations may have persisted and survived in several refugia within the Iberian Peninsula during climatic oscillations in the Pleistocene, in agreement with the "refugia-within-refugia" scenario (Gómez and Lunt, 2007; Abellán and Svenning, 2014). Our results also show that lineage F has had a long independent evolutionary history (see also Arntzen and García-París, 1995), splitting probably early in the Lower Pleistocene from other population lineages in *A. obstetricans*, and it might constitute a cryptic species. More detailed analyses of contact zones are needed to assess patterns of reproductive isolation and to clarify the taxonomic status of this divergent lineage, but its recognition as an evolutionary significant unit for conservation purposes is warranted.

In conclusion, our results evidenced a complex pattern of lineage isolation and admixture in the common midwife toad, suggesting that a mosaic of habitats in heterogeneous landscapes could be of major importance for this species to persist through changing environmental conditions. In general, the biogeographic pattern here uncovered, derived from an intense diversification process spanning the late Tertiary and Quaternary periods, supports the model of refugia-within-refugia (Gómez and Lunt, 2007), corroborating previous findings on a variety of Iberian amphibian species (Martínez-Solano et al., 2005, 2006; Sequeira et al., 2008; Gonçalves et al., 2009; Vences et al., 2013; Díaz-Rodríguez et al., 2015). Despite the influence of common environmental factors, the accumulated data have shown that temporal and spatial patterns of genetic diversity in this hotspot cannot be explained by any general model, being more consistent with idiosyncratic and organism-specific responses to driving factors of diversification. However, these idiosyncratic patterns call for meta-analyses based on hypothesis testing approaches that may clarify the importance of exogenous versus endogenous (species natural history) factors in shaping lineage and species diversity.

References

Abellán P, Svenning J-C (2014) Refugia within refugia – patterns in endemism and genetic divergence are linked to Late Quaternary climate stability in the Iberian Peninsula. *Biological Journal of the Linnean Society*, 113, 13–28.

Akaike H (1973) Information theory as an extension of the maximum likelihood principle. In: Petrov, B.N., Csaki, F. (Eds.), Second International Symposium on Information Theory. Akademiai Kiado, Budapest.

Albert EM, Fernández-Beaskoetxea S, Godoy JA, Tobler U, Schmidt BR, Bosch J (2014) Genetic management of an amphibian population after a chytridiomycosis outbreak. *Conservation Genetics*, 16, 103–111. doi:10.1007/s10592-014-0644-6

Alexandrino J, Froufe E, Arntzen JW, Ferrand N (2000) Genetic subdivision, glacial refugia and postglacial recolonization in the golden-striped salamander, *Chioglossa lusitanica* (Amphibia: Urodela). *Molecular Ecology*, 9, 771-781.

Arévalo E, Davis SK, Sites JW Jr. (1994) Mitochondrial DNA sequence divergence and phylogenetic relationships among eight chromosome races of the *Sceloporus grammicus* complex (Phrynosomatidae) in central Mexico. *Systematic Biology*, 43, 387-418.

Arntzen JW, Szymura JM (1984) Genetic differentiation between African and European midwife toads (*Alytes*, Discoglossidae). *Bijdragen tot de Dierkunde*, 54, 157–162.

Arntzen JW, García-París M (1995) Morphological and allozyme studies of midwife toads (Genus *Alytes*), including the description of two new taxa from Spain. *Contributions to Zoology*, 65, 5–34.

Avise JC (2000) Phylogeography: the history and formation of species. Cambridge, Massachusetts, Harvard University Press.

Avise JC (2009) Phylogeography: retrospect and prospect. *Journal of Biogeography*, 36, 3–15. doi:10.1111/j.1365-2699.2008.02032.x

Bosch J, Martínez-Solano I, García-París M (2001) Evidence of a chytrid fungus infection involved in the decline of the common midwife toad (*Alytes obstetricans*) in protected areas of central Spain. *Biological Conservation*, 97, 331–337.

Brunes T, Sequeira F, Haddad CFB, Alexandrino J (2010) Gene and species trees of a Neotropical group of treefrogs: genetic diversification in the Brazilian Atlantic Forest and the origin of a polyploid species. *Molecular Phylogenetics and Evolution*, 57, 1120-1133.

Crawford AJ (2003) Huge populations and old species of Costa Rican and Panamanian dirt frogs inferred from mitochondrial and nuclear gene sequences. *Molecular Ecology*, 12, 2525-2540.

Darriba D, Taboada GL, Doallo R, Posada D (2012) jModelTest 2: more models, new heuristics and parallel computing. *Nature Methods*, 9, 772.

Díaz-Rodríguez J, Gonçalves H, Sequeira F, Sousa-Neves T, Tejedo M, Ferrand N, Martínez-Solano I (2015) Molecular evidence for cryptic candidate species in Iberian *Pelodytes* (Anura, Pelodytidae). *Molecular Phylogenetics and Evolution*, 83, 224-241.

Drummond AJ, Suchard MA, Xie D, Rambaut A (2012) Bayesian phylogenetics with BEAUti and the BEAST 1.7. *Molecular Biology and Evolution,* 29, 1969–1973. doi:10.1093/molbev/mss075

Dufresnes C, Wassef J, Ghali K, Brelsford A, Stöck M, Lymberakis P, Crnobrnja-Isailović J, Perrin N (2013) Conservation phylogeography: does historical diversity contribute to regional vulnerability in European tree frogs (*Hyla arborea*)? *Molecular Ecology,* 22, 5669–5684. doi:10.1111/mec.12513

Flot J-F (2010) SeqPHASE: a web tool for interconverting PHASE input/output files and FASTA sequence alignments. *Molecular Ecology Resources*, 10, 162-166.

Fonseca A, Arntzen JW, Crespo EG, Ferrand N (2003) Regional differentiation in the common midwife toad (*Alytes obstetricans*) in Portugal: a picture from mitochondrial DNA. *Zeitschrift für Feldherpetologie*, 10, 83–89.

Fordham DA, Brook BW, Moritz C, Nogués-Bravo D (2014) Better forecasts of range dynamics using genetic data. *Trends in Ecology & Evolution*, 29, 436–443. doi:10.1016/j.tree.2014.05.007

Fu YX (1997) Statistical tests of neutrality of mutations against population growth, hitchhiking and background selection. *Genetics*, 147, 915-925.

García-París M (1995) Variabilidad genética y distribución geográfica de *Alytes obstetricans almogavarii* en España. *Revista Española de Herpetología*, 9, 133–138.

García-París M, Martínez-Solano I (2001) Nuevo estatus taxonómico para las poblaciones iberomediterráneas de *Alytes obstetricans* (Anura: Discoglossidae). *Revista Española de Herpetología*, 15, 99–113.

Geniez P, Crochet P-A (2003) Confirmation de l'existence, en France, de trois taxons méconnus: *Alytes obstetricans almogavarii* Arntzen & García-París, 1995 (Amphibia, Discoglossidae), *Podarcis hispanica sebastiani* (Klemmer, 1964) (Reptilia, Lacertidae) et *Natrix natrix astreptophora* (Seoane, 1884) (Reptilia, Colubridae). *Bulletin de la Société Herpétologique de France*, 105, 41-53.

Gómez A, Lunt DH (2007) Refugia within refugia: patterns of phylogeographic concordance in the Iberian Peninsula. Phylogeography in Southern European Refugia: Evolutionary Perspectives on the Origin and Conservation of European Biodiversity (eds. S Weiss, N Ferrand), pp. 155-188. Springer, Dordrecht, The Netherlands.

Gonçalves H, Martínez-Solano I, Ferrand N, García-París M (2007) Conflicting phylogenetic signal of nuclear *vs* mitochondrial DNA markers in midwife toads (Anura, Discoglossidae, *Alytes*): deep coalescence or ancestral hybridization? *Molecular Phylogenetics and Evolution*, 44, 494-500.

Gonçalves H, Martínez-Solano I, Pereira RJ, Carvalho B, García-París M, Ferrand N (2009) High levels of population subdivision in a morphologically conserved Mediterranean toad (*Alytes cisternasii*) result from recent, multiple refugia: evidence from mtDNA, microsatellites and nuclear genealogies. *Molecular Ecology*, 18, 5143–5160.

Grossenbacher K (1997) *Alytes obstetricans* (Laurenti, 1768). Atlas of amphibians and reptiles in Europe (eds. J-P Gasc et al.), pp. 94–95. Societas Europaea Herpetologica, Paris.

Hall TA (1999) BioEdit: a user-friendly biological sequence alignment editor and analysis program for Windows 95/98/NT. *Nucl. Acids. Symp. Ser.*, 41, 95-98.

Hampe A, Petit RJ (2005) Conserving biodiversity under climate change: the rear edge matters. *Ecology Letters*, 8, 461–467.

Heled J, Drummond AJ (2008) Bayesian inference of population size history from multiple loci. *BMC Evol Biol* 8, 289.

Heled J, Drummond AJ (2010) Bayesian inference of species trees from multilocus data. *Molecular Biology and Evolution*, 27, 570–580.

Hewitt GM (1996) Some genetic consequences of ice ages, and their role in divergence and speciation. *Biological Journal of the Linnean Society*, 58, 247–276.

Hewitt GM (2000) The genetic legacy of the Quaternary ice ages. *Nature*, 405, 907–913.

Hewitt, GM (2001) Speciation, hybrid zones and phylogeography—or seeing genes in space and time. *Molecular Ecology*, 10, 537–549.

Hewitt GM (2004) Genetic consequences of climatic oscillations in the Quaternary. *Philosophical Transactions of the Royal Society of London B, Biological Sciences*, 359, 183–195.

Huelsenbeck JP, Ronquist F (2001) MrBayes: Bayesian inference of phylogenetic trees. *Bioinformatics*, 17, 754–755.

Jockusch EL, Martínez-Solano Í, Timpe EK (2015) The effects of inference method, population sampling, and gene sampling on species tree inferences: an empirical study in slender salamanders (Plethodontidae: *Batrachoseps*). *Syst Biol,* 64, 66–83. doi:10.1093/sysbio/syu078

Lanfear R, Calcott B, Ho SYW, Guindon S (2012) PartitionFinder: combined selection of partitioning schemes and substitution models for phylogenetic analyses. *Molecular Biology and Evolution*, 29, 1695-1701.

Librado P, Rozas J (2009) DnaSP v5: a software for comprehensive analysis of polymorphism DNA data. *Bioinformatics*, 25, 1451-1452.

Maia-Carvalho B, Gonçalves H, Martínez-Solano I, Gutiérrez-Rodríguez J, Lopes S, Ferrand N, Sequeira F (2014a) Intraspecific genetic variation in the common midwife toad (*Alytes obstetricans*): subspecies assignment using mitochondrial and microsatellite markers. *Journal of Zoological Systematics and Evolutionary Research*, 52, 170-175.

Maia-Carvalho B, Gonçalves H, Ferrand N, Martínez-Solano I (2014b) Multilocus assessment of phylogenetic relationships in *Alytes* (Anura, Alytidae). *Molecular Phylogenetics and Evolution*, 79, 270-278.

Márquez R, Olmo JL, Bosch J (1995) Recurrent mass mortality of larval midwife toads *Alytes obstetricans* in a lake in the Pyrenean mountains. *Herpetological Journal*, 5, 287-289.Martínez-Solano I (2004) Phylogeography of Iberian *Discoglossus* (Anura: Discoglossidae). *Journal of Zoological Systematics and Evolutionary Research,* 42, 298–305.

Martínez-Solano I (2004) Phylogeography of Iberian *Discoglossus* (Anura: Discoglossidae). *Journal of Zoological Systematics and Evolutionary Research*, 42, 298–305.

Martínez-Solano I, Gonçalves H, Arntzen JW, García-París M (2004) Phylogenetic relationships and biogeography of midwife toads (Discoglossidae: *Alytes*). *Journal of Biogeography*, 31, 603-618.

Martínez-Solano I, Alcobendas M, Buckley D, García-París, M (2005) Molecular characterisation of the endangered *Salamandra salamandra almanzoris* (Caudata, Salamandridae). *Annales Zoologici Fennici,* 42, 57–68.

Martínez-Solano I, Teixeira J, Buckley D, García-París M (2006) Mitochondrial DNA phylogeography of *Lissotriton boscai* (Caudata, Salamandridae): evidence for old, multiple refugia in an Iberian endemic. *Molecular Ecology*, 15, 3375-3388.

Miller MA, Pfeiffer W, Schwartz T (2010) Creating the CIPRES Science Gateway for inference of large phylogenetic trees. In: Proceedings of the Gateway Computing Environments Workshop (GCE), 14 November 2010, New Orleans, LA, pp. 1–8.

Milne I, Wrigh F, Rowe G, Marshall DF, Husmeier D, McGuire G (2004) TOPALi: software for automatic identification of recombinant sequences within DNA multiple alignments. *Bioinformatics*, 20, 1806-1807.

Moritz C, Agudo R (2013) The future of species under climate change: resilience or decline? *Science,* 341, 504–508. doi:10.1126/science.1237190

Nylander JAA, Wilgenbusch JC, Warren DL, Swofford DL (2008) AWTY (are we there yet?): a system for graphical exploration of MCMC convergence in Bayesian phylogenetics. *Bioinformatics*, 24, 581–583.

Pabijan M, Wandycz A, Hofman S, Węcek K, Piwczyński M, Szymura JM (2013) Complete mitochondrial genomes resolve phylogenetic relationships within *Bombina* (Anura: Bombinatoridae). *Molecular Phylogenetics and Evolution* 69, 63–74.

Paulo OS, Dias C, Bruford MW, Jordan WC, Nichols RA (2001) The persistence of Pliocene populations through the Pleistocene climatic cycles: evidence from the phylogeography of an Iberian lizard. *Proceedings of the Royal Society of London B, Biological Sciences*, 268, 1625–1630.

Pinho C, Rocha S, Carvalho BM, Lopes S, Mourão S, Vallinoto M, Brunes TO, Haddad CFB, Gonçalves H, Sequeira F (2010). New primers for the amplification and sequencing of nuclear loci in a taxonomically wide set of reptiles and amphibians. *Conservation Genetics Resources*, 2, 181-185.

Price SJ, Garner TWJ, Nichols RA, Balloux F, Ayres C, de Alba AM-C, Bosch J (2014) Collapse of amphibian communities due to an introduced Ranavirus. *Current Biology*, 24, 2586–2591. doi:10.1016/j.cub.2014.09.028

Rambaut A, Suchard MA, Xie D, Drummond AJ (2014) Tracer v1.6, Available from http://beast.bio.ed.ac.uk/Tracer

Ramos-Onsins SE, Rozas J (2002) Statistical properties of new neutrality tests against population growth. *Molecular Biology and Evolution*, 19, 2092-2100.

Recuero E, García-París M (2011) Evolutionary history of *Lissotriton helveticus*: multilocus assessment of ancestral vs. recent colonization of the Iberian Peninsula. *Molecular Phylogenetics and Evolution,* 60, 170–182. doi:10.1016/j.ympev.2011.04.006

Rogers AR, Harpending HC (1992) Population growth makes waves in the distribution of pairwise genetic differences. *Molecular Biology and Evolution*, 9, 552-569.

Rosa GM, Anza I, Moreira PL, Conde J, Martins F, Fisher MC, Bosch J (2012). Evidence of chytrid-mediated population declines in common midwife toad in Serra da Estrela, Portugal. *Animal Conservation*, 16, 306–315. doi:10.1111/j.1469-1795.2012.00602.x

Salzburger W, Ewing GB, Von Haeseler A (2011) The performance of phylogenetic algorithms in estimating haplotype genealogies with migration. *Molecular Ecology*, 20, 1952-1963.

Sambrook J, Fritsch EF, Maniatis T (1989) *Molecular Cloning: A Laboratory Manual*, 2nd edn. Cold Spring Harbor Press, New York.

San Mauro D, García-París M, Zardoya R (2004) Phylogenetic relationships of discoglossid frogs (Amphibia: Anura: Discoglossidae) based on complete mitochondrial genomes and nuclear genes. *Gene,* 343, 357–366. doi:10.1016/j.gene.2004.10.001

Schoville SD, Bonin A, Francois O, Lobreaux S, Melodelima C, Manel S (2012) Adaptive genetic variation on the landscape: methods and cases. *Annual Review of Ecology, Evolution, and Systematics*, 43, 23–43. doi:10.1146/annurev-ecolsys-110411-160248

Sequeira F, Ferrand N, Harris DJ (2006) Assessing the phylogenetic signal on the nuclear β-fibrinogen intron 7 in salamandrids (Amphibia: Salamandridae). *Amphibia-Reptilia*, 27, 409-418.

Sequeira F, Alexandrino J, Weiss S, Ferrand N (2008) Documenting the advantages and limitations of different classes of molecular markers in a well-established phylogeographic context: lessons from the Iberian endemic Golden-striped salamander, *Chioglossa lusitanica* (Caudata: Salamandridae). *Biological Journal of the Linnean Society*, 95, 371–387.

Silvestro D, Michalak I (2010) RAxML GUI: A Graphical Front-end for RAML. <http://sourceforge.net/projects/raxmlgui/>.

Sousa-Neves T, Aleixo A, Sequeira F (2013). Cryptic patterns of diversification of a widespread Amazonian Woodcreeper species complex (Aves: Dendrocolaptidae) inferred from multilocus phylogenetic analysis: implications for historical biogeography and taxonomy. *Molecular Phylogenetics and Evolution*, 68, 410-424.

Stamatakis A (2006) RAxML-VI-HPC: maximum likelihood-based phylogenetic analyses with thousands of taxa and mixed models. *Bioinformatics*, 22, 2688–2690.

Stephens M, Smith N, Donnelly P (2001) A new statistical method for haplotype reconstruction from population data. *American Journal of Human Genetics*, 68, 978-989.

Stephens M, Donnelly P (2003) A comparison of Bayesian methods for haplotype reconstruction from population genotype data. *American Journal of Human Genetics*, 73, 1162-1169.

Stewart JR, Lister AM, Barnes I, Dalén L (2010) Refugia revisited: individualistic responses of species in space and time. *Proceedings of the Royal Society B*, 277, 661–671.

Taberlet P, Fumagalli L, Wust-Saucy AG, Cosson JF (1998) Comparative phylogeography and postglacial colonization routes in Europe. *Molecular Ecology*, 7, 453–464.

Tajima F (1989) Statistical-method for testing the neutral mutation hypothesis by DNA polymorphism. *Genetics*, 123, 585-595.

Tamura K, Peterson D, Peterson N, Stecher G, Nei M, Kumar S (2011) MEGA5: molecular evolutionary genetics analysis using maximum likelihood, evolutionary distance, and maximum parsimony methods. *Molecular Biology and Evolution*, 28, 2731-2739.

Velo-Antón G, Parra JL, Parra-Olea G, Zamudio KR (2013) Tracking climate change in a dispersal-limited species: reduced spatial and genetic connectivity in a montane salamander. *Molecular Ecology*, 22, 3261–3278. doi:10.1111/mec.12310

Vences M, Hauswaldt JS, Steinfartz S, Rupp O, Goesmann A, Künzel S, Orozco-terWengel P, Vieites DR, Nieto-Roman S, Haas S, Laugsch C, Gehara M, Bruchmann S, Pabijan M, Ludewig A-K, Rudert D, Angelini C, Borkin LJ, Crochet P-A, Crottini A, Dubois A, Ficetola GF, Galán P, Geniez P, Hachtel M, Jovanovic O, Litvinchuk SN, Lymberakis P, Ohler A, Smirnov NA (2013): Radically different phylogeographies and patterns of genetic variation in two European brown frogs, genus *Rana*. *Molecular Phylogenetics and Evolution*, 68, 657-670.

Walker SF, Bosch J, Gomez V, Garner TWJ, Cunningham AA, Schmeller DS, Ninyerola M, Henk DA, Ginestet C, Arthur C-P, Fisher MC (2010) Factors driving pathogenicity vs. prevalence of amphibian panzootic chytridiomycosis in Iberia. *Ecology Letters*, 13, 372–382. doi:10.1111/j.1461-0248.2009.01434.x

Figure Legends

Figure 1 Distribution map of *Alytes obstetricans* subspecies (dark shading, adapted from García-París and Martínez-Solano, 2001) with indication of the geographical origin of all samples analyzed in the present study (population numbers as in Table 1). Note the broad areas where subspecific assignment of populations is undetermined (light shading). Coloured circles around numbers represent the six mtDNA haplogroups recovered in the analyses. In three populations (22, 43 and 89), we found haplotypes of different haplogroups co-occurring.

Figure 2 Phylogenetic tree inferred from a Bayesian analysis of sequences of the mitochondrial *ND4* gene (813bp) in *Alytes obstetricans*. Posterior probabilities and maximum-likelihood bootstrap values of well-supported nodes (BPP≥0.9/BS≥75) are shown at nodes. Sample codes as in Table 1.

Figure 3 Haplotype genealogies from a maximum likelihood analysis of mtDNA *ND4*, and nuclear *RPL9int4*, *PPP3CAint3*, *β-fibint7* and *C-myc* genes performed with the software Haploviewer. Colours represent the different mtDNA haplogroups (as in Figs. 1 and 2, see text for details). Each circle represents a different haplotype and its size is proportional to its relative frequency (see scale). Dots represent inferred unsampled or extinct haplotypes.

Figure 4 Mismatch-distributions for each population lineage. Red curves show the expected distribution of mutations according to the null hypothesis of demographic expansion. The number of pairwise differences and their frequencies are shown on the horizontal and vertical axes, respectively.

Figure 5 Extended Bayesian Skyline Plot showing a sustained increase in effective population size (*Ne*) in *A. obstetricans* since the Pleistocene (horizontal axis, scale in millions of years). Lines represent the mean and upper and lower limits of the 95% HPDi.

Figure 6 *Alytes* species tree including all major population lineages in *Alytes obstetricans* based on the coalescent-based analysis of sequences of mtDNA *ND4* and four nuclear genes (*RPL9int4*, *PPP3CAint3*, *β-fibint7* and *C-myc*) in *BEAST. Values at nodes indicate Bayesian posterior probabilities. Bars show 95% highest posterior density intervals for split times. Scale (bottom) in millions of years.

30

Table 1 Samples analyzed in this study, with mtDNA haplogroups (see text), sample code, locality, country, population number (as in Fig. 1), latitude and longitude, and GenBank accession numbers for newly generated sequences. Sample numbers as in Figs. 2 and 3. --- : no data.

Species	mtDNA haplogroup	Sample Code	Locality	Country	Pop Nº	Sample Nº	Latitude	Longitude	GeneBank Accession nº				
									ND4	*ß-fibint7*	*C-myc*	*RPL9int4*	*PPP3CAint4*
A. obstetricans	D	SMA25	Rib. S. Bento, Serra S. Mamede	Portugal	1	1.1	39.317	-7.417	EF441303(a)	EF441330(a)	KJ859017(e)	KJ859049/KJ859050(e)	KJ859036/KJ859037(e)
		SMA26				1.2			***	---	---	***	***
		NAZ1	Valado dos Frades, Nazaré	Portugal	2	2.1	39.596	-9.020	KF626441(d)	***	---	---	---
		NAZ2				2.2			KF626442(d)	***	***	***	***
		IMS1460	Coimbra a Miranda do Corvo	Portugal	3	3.1	40.111	-8.379	***	***	---	---	---
		IMS1461				3.2			***	***	---	---	---
		EST26	Serra da Estrela	Portugal	4	4.1	40.333	-7.617	***	---	---	---	---
		EST27				4.2			***	---	---	---	---
		MAL4	Serra da Malcata	Portugal	5	5.1	40.306	-7.078	***	***	---	---	---
		MAL5				5.2			***	***	---	---	---
		GAT1	Puerto Nuevo, Sierra de Gata, Cáceres	Spain	6	6.1	40.361	-6.536	EF441301(a)	EF441327(a)	***	***	***
		GAT2				6.2			***	***	---	***	***
		GAT3				6.3			---	---	***	---	---
		IMS2928	Cabezuela del Valle, Cáceres	Spain	7	7	40.211	-5.778	***	***	---	---	---
		IMS3640	Navarredonda de Gredos, Ávila	Spain	8	8	40.330	-5.116	***	***	---	---	---
		MAN1	Freixiosa, Mangualde	Portugal	9	9	40.600	-7.683	***	***	---	---	---
		VOU8	Rio Mau, Sever do Vouga	Portugal	10	10.1	40.733	-8.400	---	***	---	---	---

31

	VOU11				10.2			***	---	---	---	---
	FCO2	Penedono, V.N. Foz Côa	Portugal	11	11	40.983	-7.400	***	---	---	---	---
	MTM1	Cinfães, Serra de Montemuro	Portugal	12	12.1	41.078	-8.024	EF441302(a)	EF441328/ EF441329(a)	***	---	***
	MTM2				12.2			***	KJ859006/ KJ859007(e)	***	***	***
	MTM5				12.3			---	---	KJ859018(e)	KJ859051(e)	KJ859038(e)
C	VAL22	Alfena, Valongo	Portugal	13	13.1	41.240	-8.525	EF441300(a)	EF441325/ EF441326(a)	***	***	***
	VAL24				13.2			***	---	---	---	---
	LOU2	Lousada	Portugal	14	14.1	41.303	-8.253	***	***	---	---	---
	LOU6				14.2			***	***	---	---	---
	VPA5	Cerva, Serra do Alvão	Portugal	15	15.1	41.467	-7.833	---	***	---	---	---
	VPA6				15.2			---	***	---	---	---
	VPA9				15.3			***	---	---	---	---
	VPA13				15.4			***	---	---	---	---
	MUR1	Jou, Murça	Portugal	16	16	41.483	-7.433	***	***	---	---	---
	GER1	Carris, Serra do Gerês	Portugal	17	17.1	41.817	-8.050	***	***	***	***	***
	GER2				17.2			***	***	---	---	---
	VER1	Castrelo del Valle, Verín, Pontevedra	Spain	18	18.1	41.983	-7.417	***	***	---	---	---
	VER2				18.2			***	***	---	***	***
	LUG1	Fontaneira, Lugo	Spain	19	19.1	43.034	-7.200	***	***	***	***	***
	LUG2				19.2			***	---	---	---	---
	OUR2	Penalba, Ourense	Spain	20	20.1	43.425	-7.733	***	***	---	---	---
	OUR3				20.2			EF441295(a)	EF441319(a)	KJ859016(e)	GU181180(c)	GU181147(c)/ KJ859035(e)
	PON1	Monte Aloia, Tuy, Pontevedra	Spain	21	21.1	42.050	-8.633	EF441296(a)	EF441320(a)	***	***	***

32

Group	Code	Locality	Country			Lat	Long					
	MNCN8590				21.2			***	***	---	---	---
	IMS3624				21.3			***	---	---	---	---
	IMS3625				21.4			***	---	---	---	---
	IMS3626				21.5			***	---	---	---	---
	IMS3627				21.6			***	---	---	---	---
	IMS3628				21.7			***	---	---	---	---
	COR1	Arteixo, A Coruña	Spain	22	22.1	43.375	-8.433	***	***	---	---	---
B	COR2				22.2			***	***	---	---	---
	IMS2630	Alfonxe, Lugo	Spain	23	23.1	42.924	-7.389	***	***	---	---	---
	IMS2631				23.2			***	***	---	---	---
	TIN1	Tineo, Asturias	Spain	24	24	43.333	-6.417	***	***	---	***	***
	MNCN4785	Somiedo, Asturias	Spain	25	25.1	43.070	-6.306	***	***	---	---	---
	MNCN4786				25.2			***	***	---	---	---
	LEO3	Veguellina de Órbigo, León	Spain	26	26	42.450	-5.885	***	***	---	---	---
	TLV1	Tolivia, Asturias	Spain	27	27	43.200	-5.583	EF441299(a)	EF441318(a)	---	---	---
	LEO1	Lago de Isoba, León	Spain	28	28.1	43.046	-5.315	***	***	---	***	---
	LEO2				28.2			***	***	---	***	---
	LEO4				28.3			---	---	***	---	---
	MNCN8444				28.4			***	***	---	---	---
	OVI1	Puerto de San Isidro, Asturias			28.5	43.050	-5.325	***	***	---	---	---
	RIB1	El Fito, Asturias	Spain	29	29	43.433	-5.148	***	***	---	---	---
	IMS3621	Casavegas, La Pernía, Palencia	Spain	30	30	43.022	-4.513	***	---	---	---	---
	SAN4	Fresnedo, Cantabria	Spain	31	31	43.367	-3.567	***	***	---	---	---

33

	Code	Locality	Country	No	Sub	Lat	Long					
	SAN1		Spain	32	32.1	43.350	-3.333	***	KJ859005(e)	KJ859013(e)	***	***
	SAN2				32.2			***	***	---	---	---
	SAN3				32.3			***	***	---	---	---
	IMS3009	P.N. Gorbeia, Vizcaya	Spain	33	33.1	43.088	-2.792	***	---	---	---	---
	IMS3010				33.2			***	***	---	---	---
	MNCN4445	Sierra de Andía, Navarra	Spain	34	34	42.818	-1.970	***	---	---	---	---
	IMS4096	Ribaforada, Navarra	Spain	35	35	42.006	-1.536	***	---	---	---	---
	PAM1	Irati, Navarra	Spain	36	36.1	42.993	-1.100	***	***	***	***	***
	PAM2				36.2			EF441293(a)	EF441317(a)	---	---	---
	IMS3959	Iraty Lake	France	37	37	43.046	-1.074	***	---	---	---	---
	FRAN10	Saint-Michel	France	38	38	43.168	1.084	***	---	---	---	---
	FRAN3	La Sallète	France	39	39	43.993	2.167	***	***	---	---	---
	FRAN14	St Pierre-de-la-Fage	France	40	40	43.794	3.420	---	---	---	KJ859048(e)	KJ859034(e)
	FRAN1	Jublains	France	41	41.1	48.251	-0.501	EF441292(a)	EF441316(a)	KJ859014/ KJ859015(e)	GU181178(c)	GU181145(c)
	FRAN2				41.2			***	***	---	---	---
	FRAN4				41.3			---	---	***	---	---
	GERM1	Rhür Valley	Germany	42	42	51.517	7.450	EF441291(a)	EF441315(a)	---	---	---
	TUD2	Tudanca, Cantabria	Spain	43	43.1	43.150	-4.367	***	***	---	---	---
	TUD3				43.2			***	---	---	---	---
	TUD4				43.3			***	---	---	---	---
A	TUD1				43.4			***	***	---	***	***
	IMS3507	Feces de Abaixo	Portugal	44	44	41.810	-7.422	***	---	---	---	---
	MON1	Refega, Serra de Montesinho	Portugal	45	45.1	41.783	-6.583	***	***	---	---	---

34

Code	Locality	Country			Lat	Long					
MON12				45.2			***	***	---	---	---
MON15				45.3			***	***	---	---	---
MIR1	Mirandela	Portugal	46	46	41.483	-7.167	***	***	---	---	---
MOG5	Mogadouro	Portugal	47	47.1	41.333	-6.717	***	***	---	---	---
MOG6				47.2			***	***	---	---	---
CAC1	Arroyo San Blas, Sierra de Gata, Cáceres	Spain	48	48.1	40.233	-6.600	***	***	---	---	---
CAC2				48.2			---	***	---	---	---
ZAM1	Valdefinjas, Zamora	Spain	49	49.1	41.451	-5.451	***	***	---	---	---
ZAM2				49.2			EF441297(a)	EF441321(a)	---	---	---
ZAM3				49.3			---	***	---	---	---
ZAM4				49.4			---	***	---	---	---
ZAM5				49.5			---	***	---	---	---
IMS3244				49.6			***	***	---	---	---
IMS3245				49.7			***	***	---	---	---
IMS4301	Vegas de Matute, Segovia	Spain	50	50.1	40.801	-4.258	***	---	---	---	---
IMS4302				50.2			***	---	---	---	---
IMS2749	Valsaín, Segovia	Spain	51	51.1	40.804	-4.023	***	***	---	---	---
IMS2750				51.2			***	***	---	---	---
GUA1	Pto. Cotos, Sierra de Guadarrama, Madrid			51.3	40.824	-3.962	***	***	---	***	---
GUA2				51.4			***	***	---	***	***
IMS2669	Circo del Nevero, Madrid	Spain	52	52.1	40.979	-3.844	***	***	---	---	---
IMS2670				52.2			***	***	---	---	---
IMS4055	Villaverde de Montejo, Segovia	Spain	53	53	41.504	-3.666	***	---	---	---	---

TOL1	La Guardia, Toledo	Spain	54	54.1	39.783	-3.483	***	***	---	---	---
TOL2				54.2			***	***	---	---	---
MAD1	Colmenar de Oreja, Madrid	Spain	55	55.1	40.108	-3.387	***	***	---	---	---
MAD4	Belmonte de Tajo, Madrid			55.2	40.133	-3.339	EF441298(a)	EF441322/ EF441323(a)	---	KJ859047(e)	KJ859033(e)
MAD2	Valdelaguna, Madrid			55.3	40.162	-3.368	***	***	---	---	---
MAD3				55.4			***	***	---	---	---
IMS2538	Valdaracete, Madrid	Spain	56	56	40.160	-3.179	***	***	---	---	---
GLJ2	Torija, Guadalajara	Spain	57	57.1	40.744	-3.030	***	***	---	***	***
GLJ3				57.2			***	***	***	***	***
GLJ1	Ciruelas, Guadalajara			57.3	40.752	-3.090	***	***	---	---	---
IMS2620	Gárgoles, Guadalajara	Spain	58	58.1	40.757	-2.631	***	---	---	---	---
IMS2621				58.2			***	***	---	---	---
IMS2571	Canredondo, Guadalajara			58.3	40.784	-2.544	***	***	---	---	---
IMS2572				58.4			***	***	---	---	---
IMS4358	Mirabueno, Guadalajara	Spain	59	59.1	40.948	-2.729	***	---	---	---	---
IMS4359				59.2			***	---	---	---	---
IMS3022	Cañamares, Guadalajara	Spain	60	60	41.227	-2.956	***	***	---	---	---
SOR1	Vinuesa, Soria	Spain	61	61	41.912	-2.763	***	***	---	---	---
IMS3866	Arnedo, La Rioja	Spain	62	62	42.224	-2.076	***	---	---	---	---
OLV1	Ólvega, Soria	Spain	63	63	41.781	-1.985	***	***	---	---	---
IMS2267	Moros, Zaragoza	Spain	64	64.1	41.402	-1.820	***	***	---	---	---
IMS2268				64.2			***	***	---	---	---
IMS2247	Montuenga, Soria	Spain	65	65.1	41.225	-2.210	***	---	---	---	---

36

IMS2248				65.2			***	---	---	---	---
IMS2665	Terzaga a Peralejos de las Truchas, Guadalajara	Spain	66	66.1	40.647	-1.907	***	***	---	---	---
IMS2666				66.2			***	***	---	---	---
IMS2643	Nacimiento río Tajo, Teruel	Spain	67	67.1	40.321	-1.698	***	***	---	---	---
IMS2644				67.2			***	***	---	---	---
IMS2641	Frías de Albarracín, Teruel			67.3	40.362	-1.615	***	***	---	---	---
IMS2642				67.4			***	***	---	---	---
IMS2645	Guadalaviar, Teruel			67.5	40.395	-1.728	***	***	---	---	---
IMS2646				67.6			***	---	---	---	---
CUE1	Buenache de la Sierra, Cuenca	Spain	68	68	40.134	-2.000	EF441299(a)	EF441324(a)	---	GU181179(c)	GU181146(c)
IMS2288	Tobed, Zaragoza	Spain	69	69.1	41.340	-1.399	***	***	---	---	---
IMS2289				69.2			***	***	---	---	---
IMS2633	Albarracín, Teruel	Spain	70	70.1	40.394	-1.416	***	***	---	---	---
IMS2634				70.2			***	***	---	---	---
IMS2522	Hayedo de Tejera Negra, Guadalajara	Spain	71	71	41.237	-3.350	***	***	---	---	---
IMS2299	Belchite, Zaragoza	Spain	72	72.1	41.285	-0.776	***	***	---	---	---
IMS2300				72.2			***	***	---	---	---
IMS2126	Corbalán, Teruel	Spain	73	73.1	40.406	-0.986	***	---	---	---	---
IMS2127				73.2			***	***	---	---	---
ALB1	Higueruela, Albacete	Spain	74	74.1	38.950	-1.450	***	***	---	---	***
ALB2				74.2			***	---	---	***	---
IMS1851	Las Fuentes, Albacete	Spain	75	75.1	39.003	-1.304	***	***	---	---	---
IMS1852				75.2			***	***	---	---	---

ALI1	El Pinoso, Alicante	Spain	76	76.1	38.400	-1.033	***	---	---	***	---
ALI2				76.2			***	---	---	---	---
ALI3				76.3			---	***	---	***	***
ALI4				76.4			---	***	---	---	---
IMS1932	Mas de Celedons, Alicante	Spain	77	77.1	38.669	-0.525	***	***	---	---	---
IMS1933				77.2			***	---	---	---	---
IMS1901	Enguera, Valencia	Spain	78	78.1	38.929	-0.855	***	***	---	---	---
IMS1902				78.2			***	---	---	---	---
IMS2006	Las Nogueras, Valencia	Spain	79	79.1	39.588	-1.082	***	***	---	---	---
IMS2007				79.2			***	***	---	---	---
IMS2021	Alcublas, Valencia	Spain	80	80.1	39.815	-0.700	***	***	---	---	---
IMS2022				80.2			***	***	---	---	---
VLC1	Algar de Palancia, Valencia	Spain	81	81.1	39.782	-0.367	***	---	***	---	---
VLC2				81.2			***	***	KJ859009/ KJ859010(e)	***	***
CAS1	Barranco de Santa Agueda, Benicassim, Castellón	Spain	82	82.1	40.050	0.066	***	***	---	***	---
CAS2				82.2			***	***	---	---	---
IMS2071	Barranc dels Horts, Castellón	Spain	83	83.1	40.414	-0.066	***	***	---	---	---
IMS2072				83.2			***	***	---	---	---
IMS2091	Cantavieja, Teruel	Spain	84	84.1	40.516	-0.459	***	---	---	---	---
IMS2092				84.2			***	***	---	---	---
IMS2317	Mazaleón, Teruel	Spain	85	85.1	41.061	0.110	***	---	---	---	---
IMS2318				85.2			***	---	---	---	---
IMS2314	Caspe, Zaragoza	Spain	86	86.1	41.148	0.013	***	***	---	---	---

Group	Code	Locality	Country	No.	Sub	Lat	Long					
	IMS2315				86.2			***	***	---	---	---
	IMS2367	Riudoms, Tarragona	Spain	87	87.1	41.148	1.043	***	***	---	---	---
	IMS2368				87.2			***	***	---	---	---
	IMS2337	El Perelló, Tarragona	Spain	88	88.1	40.858	0.670	***	***	---	---	---
	IMS2338				88.2			***	***	---	---	---
	IMS2387	El Port d'Armentera, Tarragona	Spain	89	89.1	41.387	1.359	***	***	---	---	---
F	IMS2388				89.2			***	---	---	---	---
	IMS2407	Piera, Barcelona	Spain	90	90.1	41.511	1.737	***	***	---	---	---
	IMS2408				90.2			***	---	---	---	---
	BAR1	Collserola, Barcelona	Spain	91	91	41.419	2.099	---	---	---	***	***
	IMS2427	Sant Miquel del Fai, Barcelona	Spain	92	92.1	41.716	2.193	***	***	---	---	---
	IMS2428				92.2			***	---	---	---	---
	IMS2447	Sant Hilari Sacalm, Girona	Spain	93	93.1	41.903	2.506	***	***	---	---	---
	IMS2448				93.2			***	---	---	---	---
	MNCN4334	Riudarenes, Girona	Spain	94	94	41.822	2.717	***	***	---	---	---
	IMS2467	La Bisbal, Girona	Spain	95	95.1	41.939	2.949	***	***	---	---	---
	IMS2468				95.2			***	***	---	---	---
	IMS2492	Prades, Lleida	Spain	96	96.1	41.795	1.579	***	---	---	---	---
	IMS2493				96.2			***	***	---	---	---
	BER5	Llinars, Lleida	Spain	97	97.1	42.131	1.709	***	***	***	***	***
	BER10				97.2			***	***	---	---	---
	BER11				97.3			***	***	---	---	---
	BER12				97.4			***	***	---	---	---

	Code	Locality	Country	No	Sub	Lat	Long					
	BER13				97.5			***	***	---	***	***
	BER14				97.6			KF626443(d)	***	***	---	---
	BER15				97.7			KF626444(d)	***	***	---	---
	BER16				97.8			***	***	---	---	---
	BER6				97.9			EF441308(a)	EF441337(a)	---	---	---
	BER7				97.10			***	---	---	---	---
	BER1	Rasos de Peguera, Berga, Barcelona			97.11	42.136	1.761	EF441305(a)	EF441332/EF441333(a)	KJ859019/KJ859020(e)	GU181177(c)/KJ859052(e)	GU181144(c)
	BER2				97.12			***	***	---	---	---
	BER3				97.13			EF441306(a)	EF441334/EF441335(a)	KJ859021(e)	KJ859053(e)	KJ859039/KJ859040(e)
	BER4				97.14			EF441307(a)	EF441336(a)	***	***	***
	BER8				97.15			***	***	---	---	---
	BER9				97.16			***	***	***	---	***
	BER20	La Coma, Berga, Barcelona	Spain	98	98.1	42.188	1.581	***	***	***	***	***
	BER21				98.2			***	***	---	---	---
	BER22				98.3			***	***	---	---	---
	BER23				98.4			***	***	---	---	---
	BER17	Soldes, Túnel del Cadí, Berga, Barcelona	Spain	99	99.1	42.350	1.700	---	***	---	---	---
	BER18				99.2			***	***	***	***	***
	BER19				99.3			***	***	---	---	---
	IMS4107	Tuchan	France	100	100	42.885	2.733	***	---	---	---	---
	BEN1	Fonchanina, Huesca	Spain	101	101	42.522	0.652	***	***	---	---	---
E	IMS2501	Naval, Huesca	Spain	102	102.1	42.188	0.154	***	***	---	---	---
	IMS2502				102.2			***	---	---	---	---

40

Species	Code	Locality	Country			Lat	Long					
	HUE1	Ibón de Piedrafita, Huesca	Spain	103	103.1	42.700	-0.333	EF441304(a)	EF441331(a)	KJ859022(e)	---	---
	HUE2				103.2			***	***	---	---	***
	HUE4				103.3			---	---	---	***	***
A. cisternasii	CER17	Cercal	Portugal	-	-	37.750	-8.650	EF441314(a)	---	---	---	---
A. cisternasii	CER01	Cercal	Portugal	-	-	37.750	-8.650	---	EF441343(a)	---	KJ859062(e)	GU086791(b)
A. cisternasii	HG113	Río Adaja, Ávila	Spain	-	-	40.650	-4.700	---	---	***	---	---
A. dickhilleni	IMS3489	Puerto de las Crucetillas, Albacete	Spain	-	-	38.545	-2.383	***	---	---	---	---
A. dickhilleni	HG103	Puerto de las Crucetillas, Sierra de Alcaraz, Albacete	Spain	-	-	38.545	-2.383	---	EF441338(a)	---	GU181176(c)	GU181143(c)
A. dickhilleni	HG104	Puerto de las Crucetillas, Sierra de Alcaraz, Albacete	Spain	-	-	38.545	-2.383	---	---	KJ859026/ KJ859025(e)	---	---
A. muletensis	IMS3517	Captivity	Spain	-	-	-	-	***	---	---	---	---
A. maurus	MAR01	Bab Bou Idir, Taza	Morocco	-	-	34.060	-4.110	***	---	---	---	---
A. maurus	MAR04	Bab Bou Idir, Taza	Morocco	-	-	34.060	-4.110	---	---	---	KJ859056(e)	KJ859043(e)
A. maurus	MAR06	Bab Bou Idir, Taza	Morocco	-	-	34.060	-4.110		---	***		
A. muletensis	MAI06	Sierra de Tramuntana, Mallorca	Spain	-	-	39.580	2.500	---	---	KJ859029(e)	GU181175(c)	GU181142(c)

(a) Gonçalves et al. (2007); (b) Gonçalves et al. (2009); (c) Pinho et al. (2010); (d) Maia-Carvalho et al. (2014a); (e) Maia-Carvalho et al. (2014b)

41

Table 2 Summary statistics for the five molecular markers sequenced in *A. obstetricans* in this study. (N) number of sequences; (S) number of segregating sites; (H) number of haplotypes; (Hd) haplotype diversity; (π) nucleotide diversity. High levels of genetic diversity were found in *A. obstetricans*. Significant values of Fu's Fs and Ramos-Onsins & Rozas' R2 statistics were obtained for the population lineages corresponding to mtDNA haplogroups A, C and D (* P<0.05; ** P<0.01), suggesting demographic expansions.

Marker	Haplogroups	N	S	H	Hd	π	Tajima's D	Fu's Fs	R_2
ND4 (813 bp)		210	127	88	0.975±0.004	0.0243±0.0012	-0.475	-24.076**	0.0765
	A	95	37	34	0.942±0.010	0.0042±0.0003	-1.657	-23.384**	0.0433*
	B	33	24	18	0.936±0.027	0.0063±0.0005	-0.467	-5.691*	0.0960
	C	23	19	10	0.640±0.116	0.0024±0.0007	-2.262**	-4.111*	0.0512**
	D	19	15	13	0.877±0.074	0.0029±0.0007	-1.681	-8.883**	0.0665**
	E	4	0	1	-	-	-		-
	F	36	15	12	0.787±0.064	0.0029±0.0004	-1.119	-3.788*	0.0778
β-fibint7 (630 - 635 bp)		338	57	108	0.971±0.004	0.0155±0.0003	0.175	-73.961**	0.0857
C-myc (1257 - 1261 bp)		60	24	18	0.904±0.024	0.0035±0.0002	-0.713	-3.446	0.0892
PPP3CAint4 (597 - 604 bp)		76	22	21	0.900±0.017	0.0075±0.0004	-0.486	-4.508	0.1003
RPL9int4 (442 - 460 bp)		82	27	26	0.908±0.023	0.0124±0.0007	-0.188	-6.392*	0.1014

Table 3 Average genetic distances (p-uncorrected) within (on the diagonal, including average and range) and between the main mtDNA haplogroups in *Alytes obstetricans*.

mtDNA haplogroup	A	B	C	D	E	F
A	0.004 (0.001 - 0.012)	0.015	0.016	0.040	0.033	0.045
B		0.007 (0.001 - 0.012)	0.014	0.043	0.033	0.045
C			0.007 (0.001 - 0.023)	0.044	0.036	0.045
D				0.003 (0.001 - 0.009)	0.039	0.052
E					0.00	0.046
F						0.003 (0.001 - 0.01)
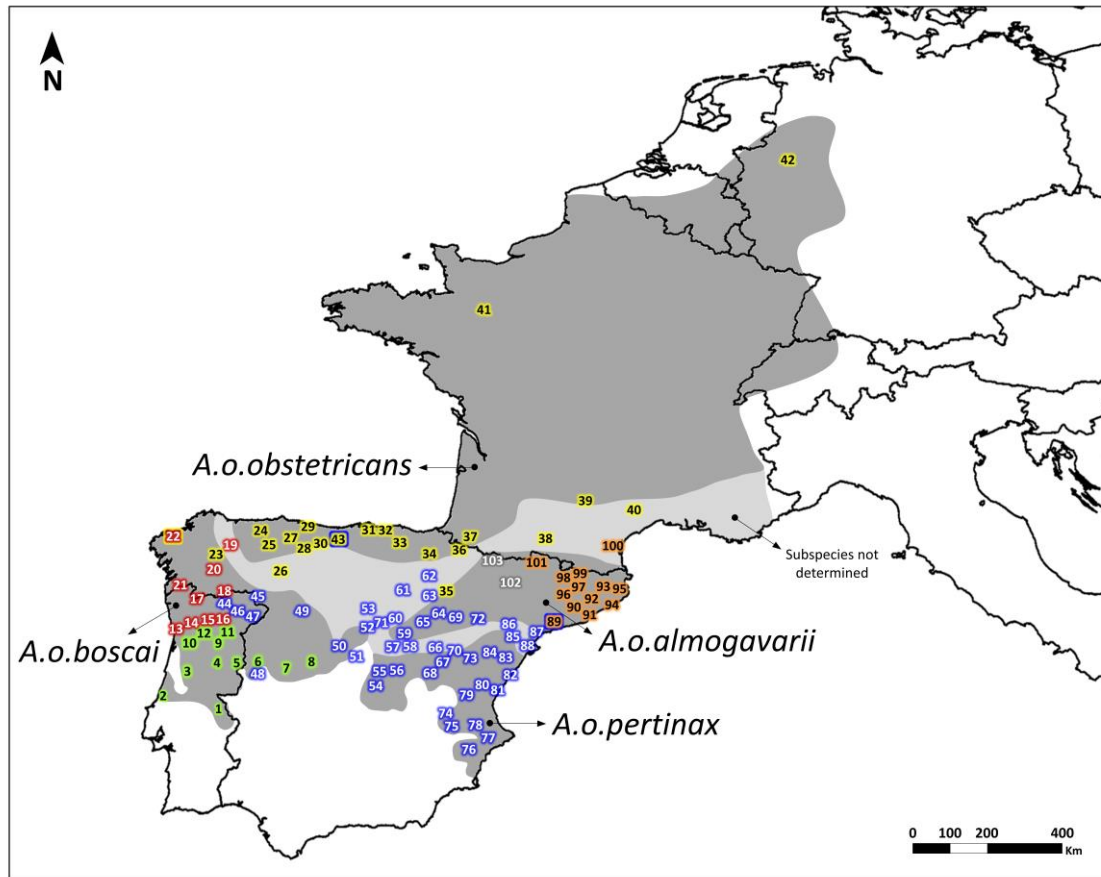
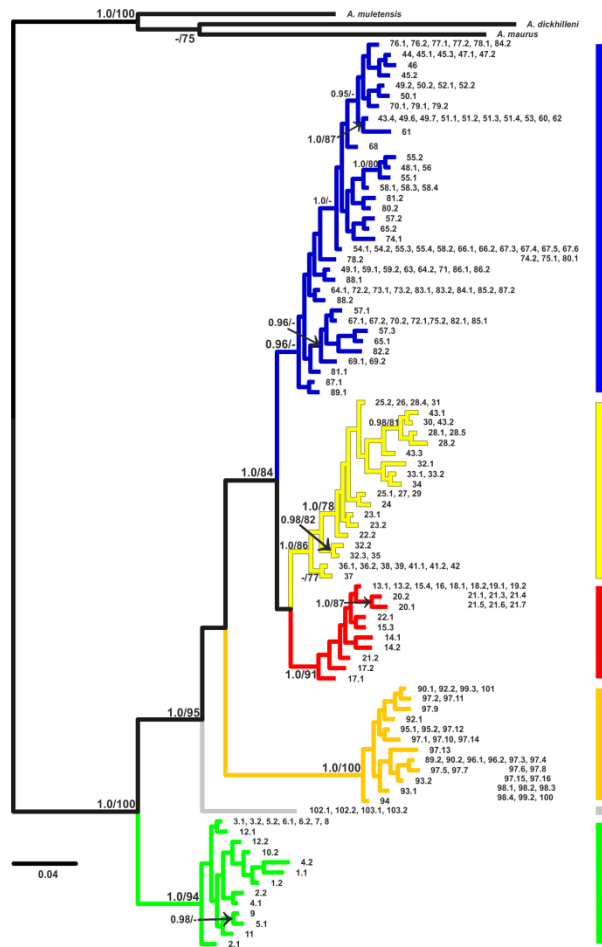**Figure 1**
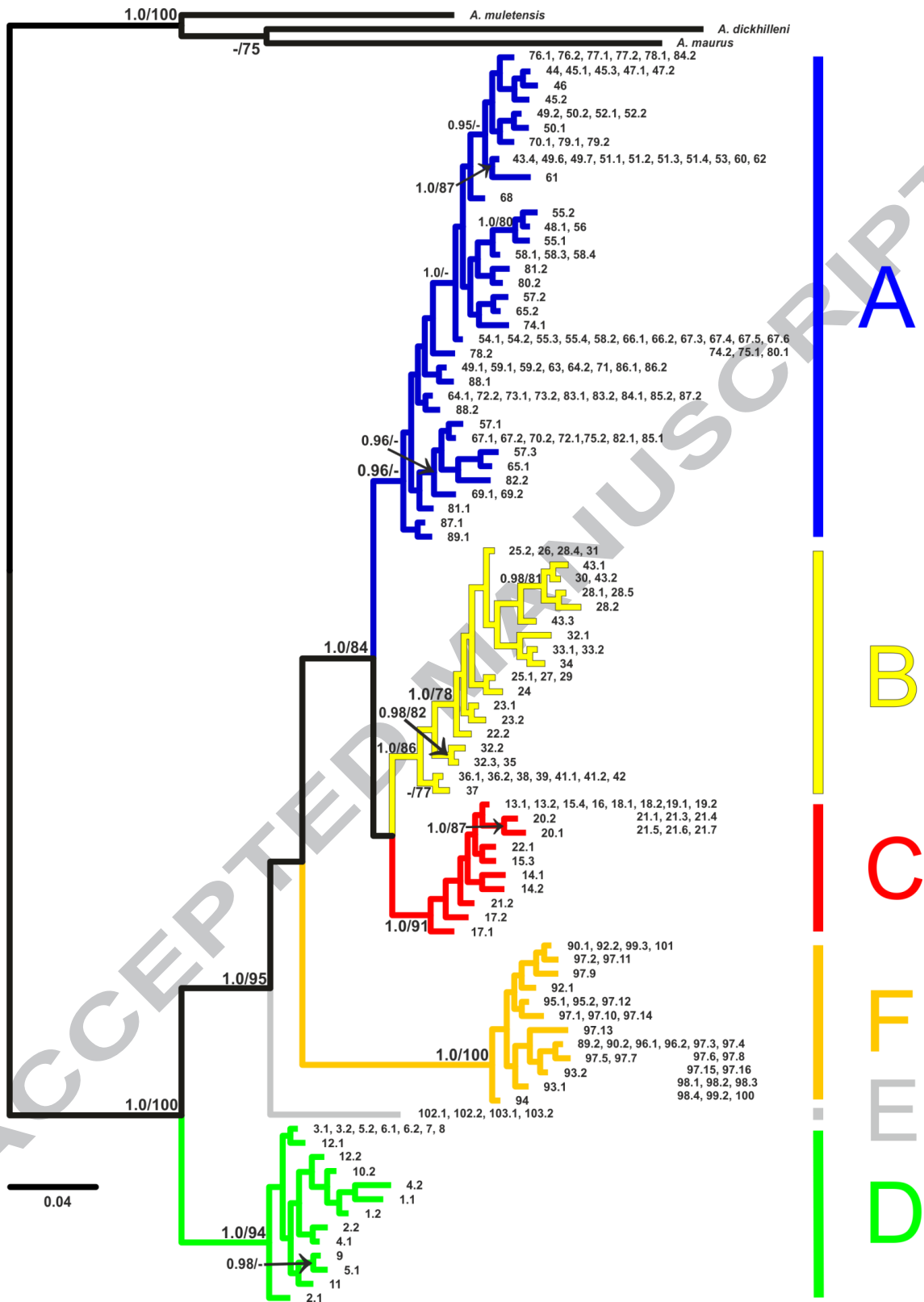
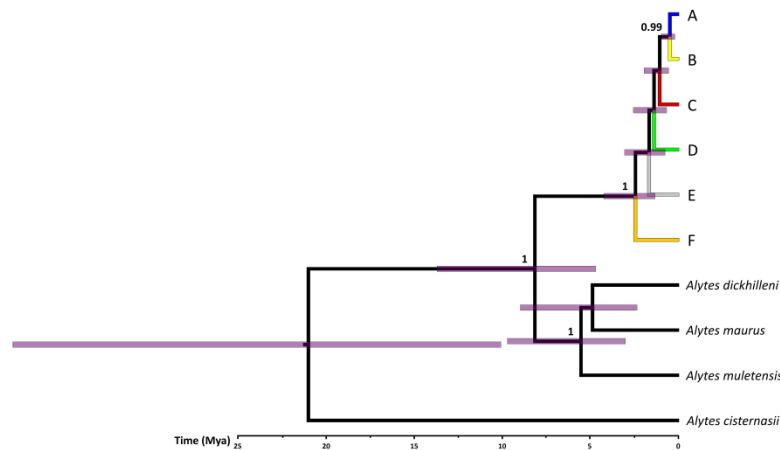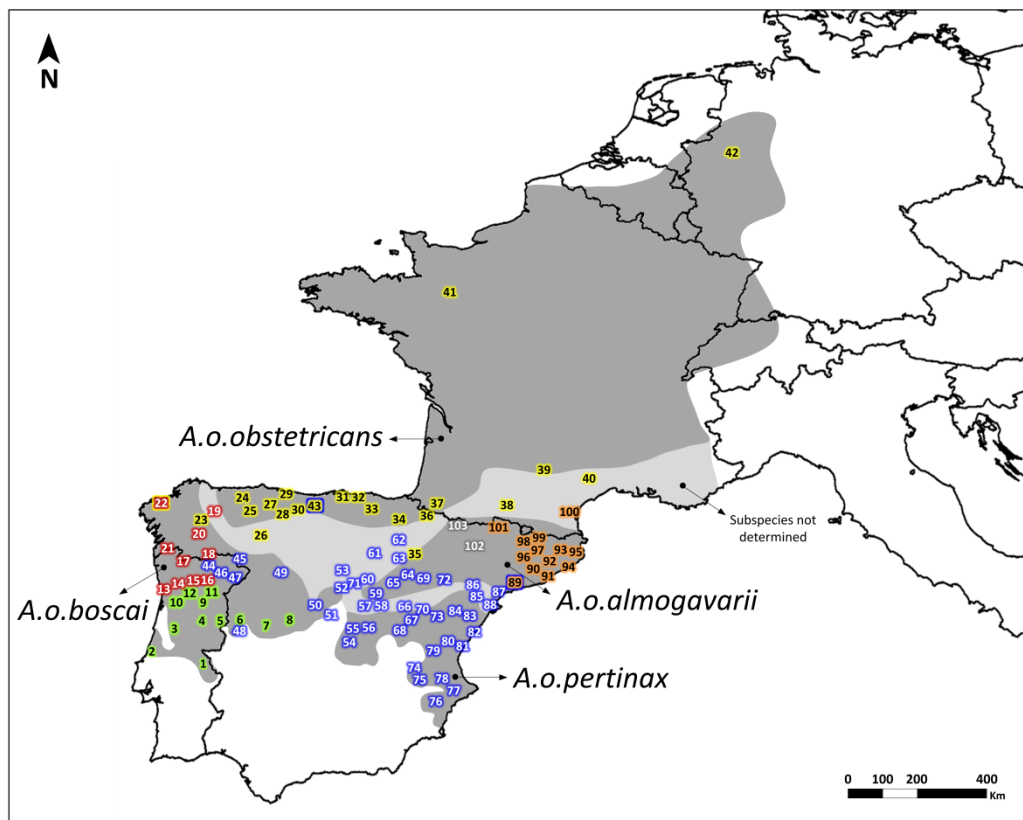**Figure 2**
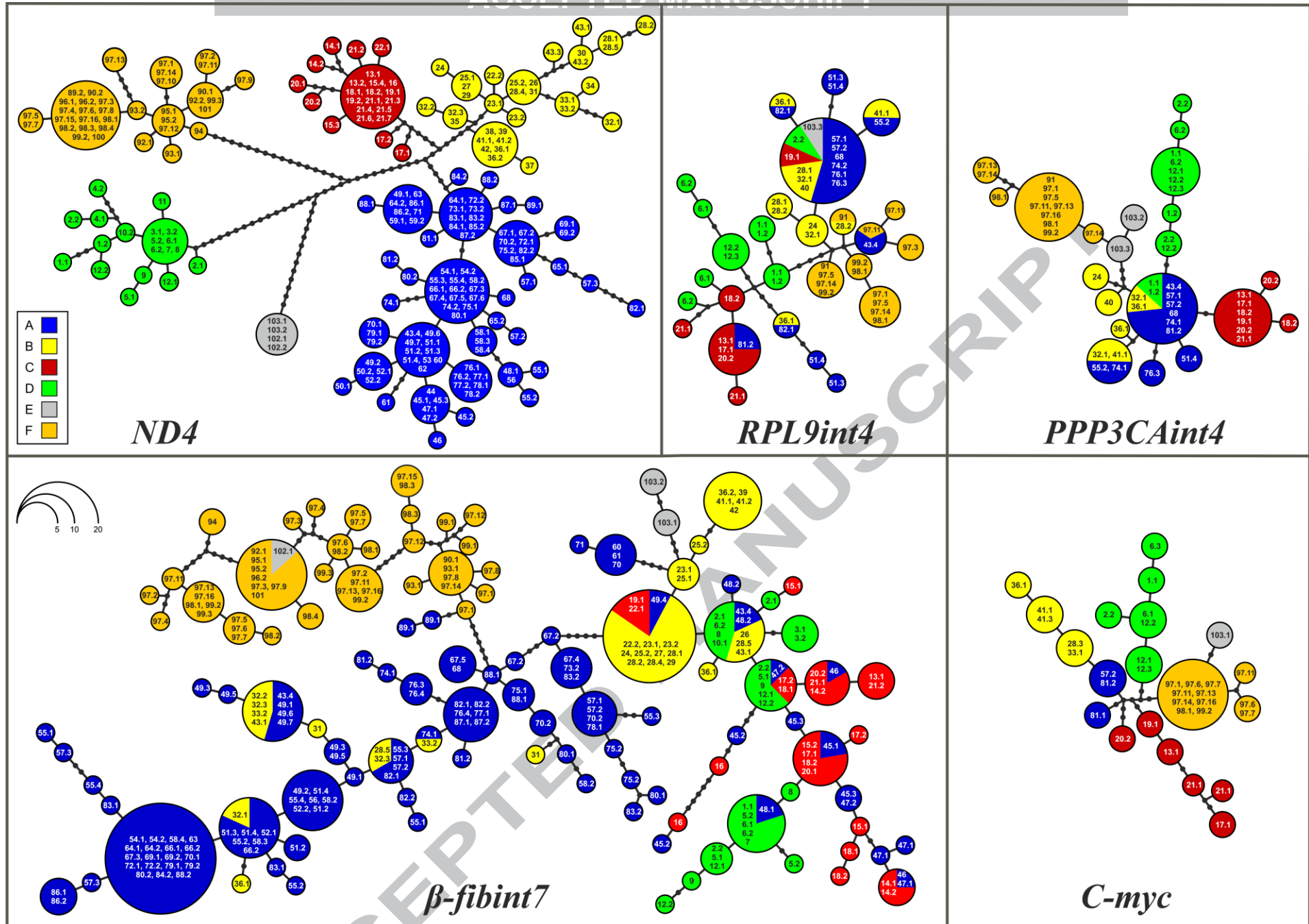
Figure 3
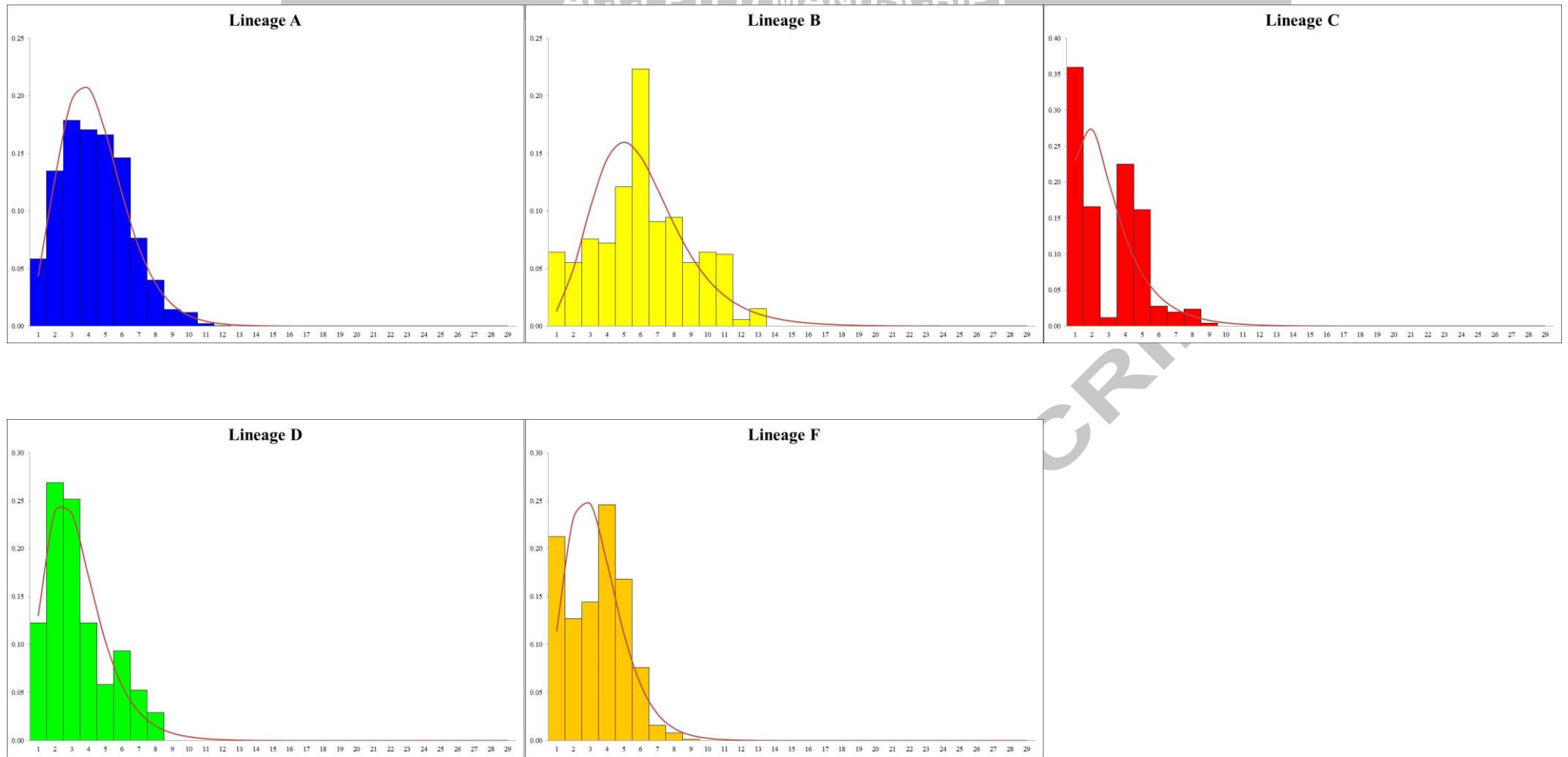
Figure 4
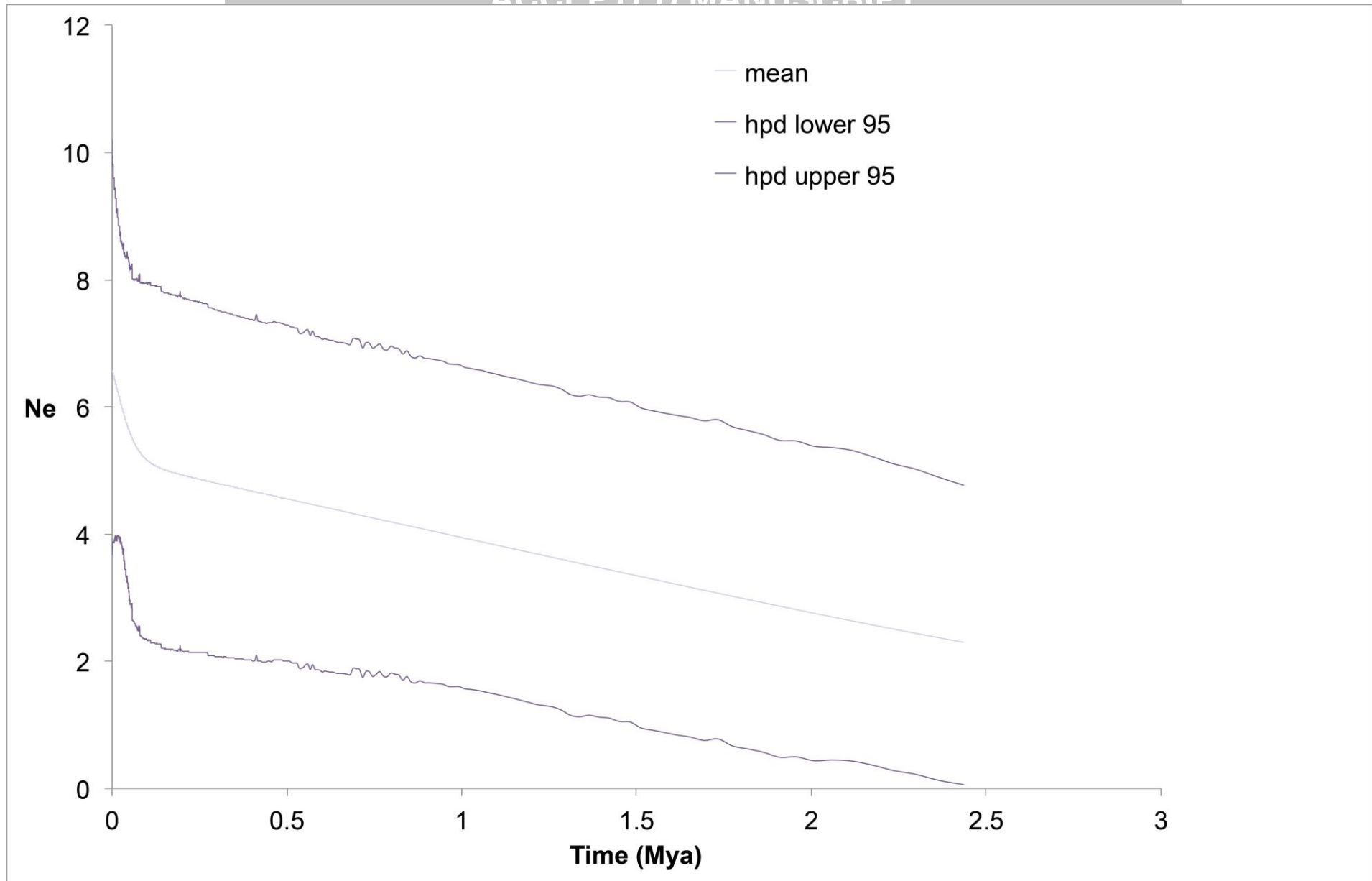
Figure 5
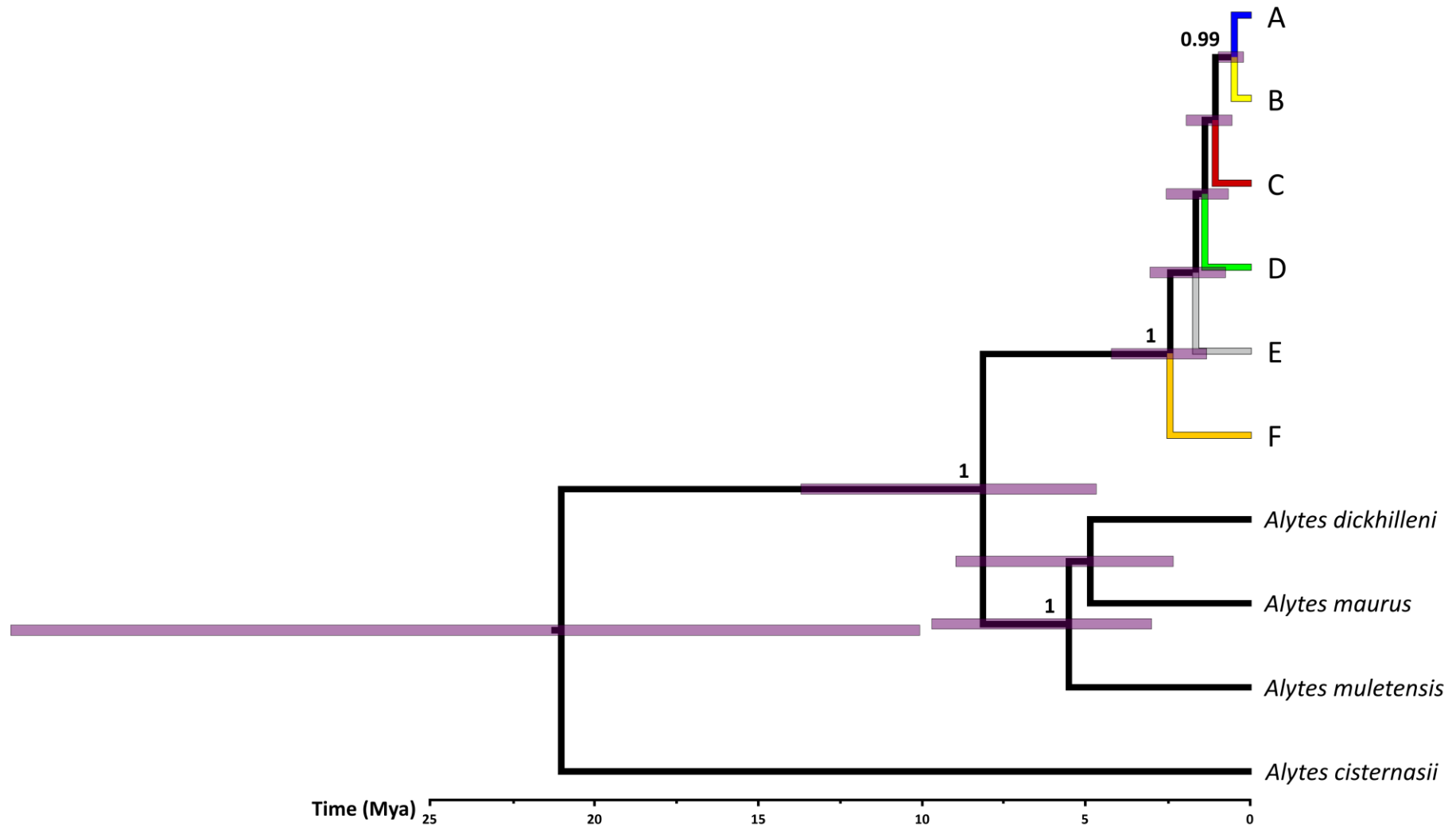
Figure 6

Highlights

- Phylogenetic analyses recover 6 mtDNA haplogroups diagnosing lineages in *A. obstetricans*

- Strong geographic structure and contrasting demographic histories across lineages

- Split times between lineages date back to the Pleistocene

- *A. o. almogavarii* shows high genetic variation and may represent a cryptic species